

AD-A068 252

SYSTEMS RESEARCH LABS INC DAYTON OHIO

F/G 11/6

AN ANALYSIS OF THE LOW CYCLE FATIGUE BEHAVIOR OF THE SUPERALLOY--ETC(U)

NOV 78 J M HYZAK, H L BERNSTEIN

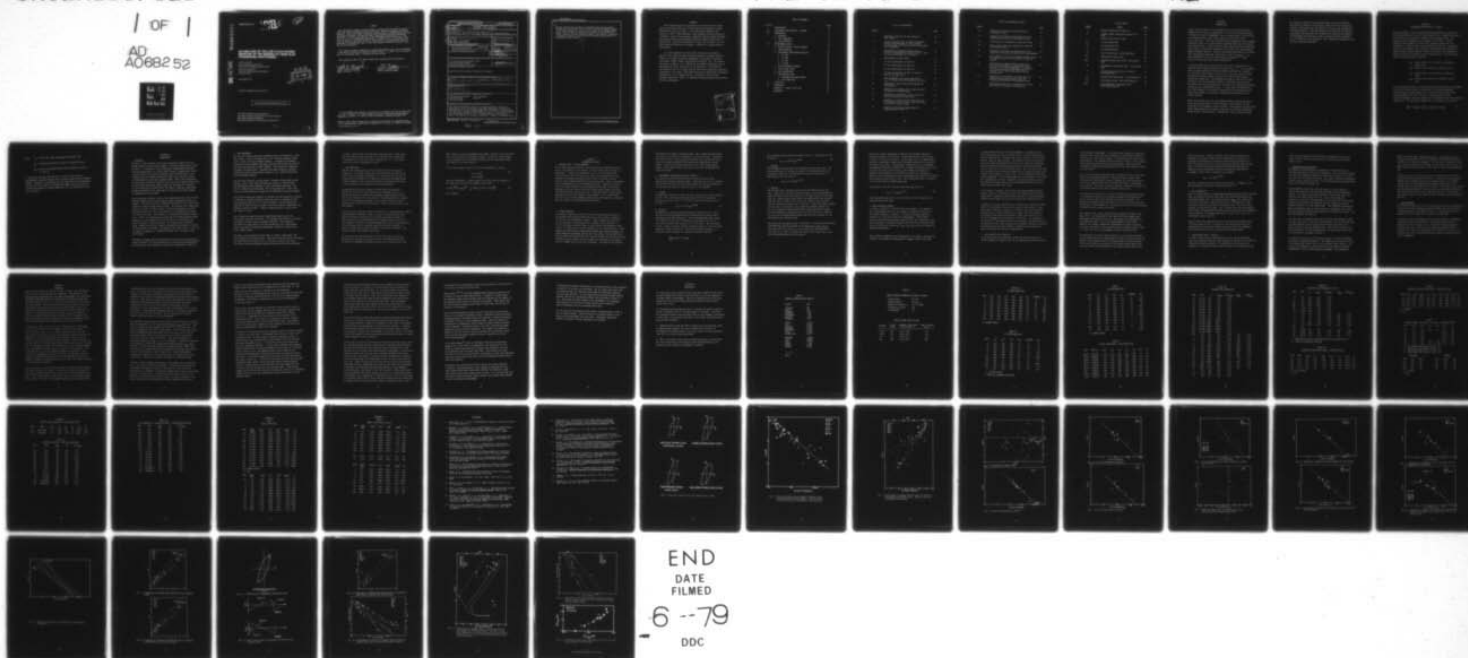
F33615-76-C-5191

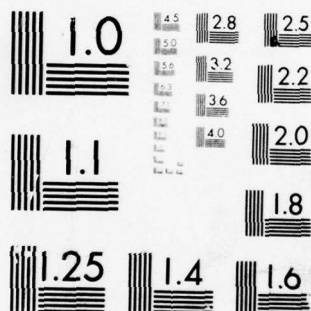
AFML-TR-78-174

NL

UNCLASSIFIED

1 OF 1
AD
A0682 52





MICROCOPY RESOLUTION TEST CHART
NATIONAL BUREAU OF STANDARDS-1963-A

AD A068252

DDC FILE COPY

AFML-TR-78-174

LEVEL II

22

AN ANALYSIS OF THE LOW CYCLE FATIGUE BEHAVIOR OF THE SUPERALLOY RENE 95 BY STRAINRANGE PARTITIONING

JACK M. HYZAK
METALS BEHAVIOR BRANCH
AIR FORCE MATERIALS LABORATORY
HENRY L. BERNSTEIN
SYSTEMS RESEARCH LABORATORIES
DAYTON, OHIO

NOVEMBER 1978

DDC
RECEIVED
MAY 7 1979
C

TECHNICAL REPORT AFML-TR-78-174

Approved for public release; distribution unlimited.

AIR FORCE MATERIALS LABORATORY
AIR FORCE WRIGHT AERONAUTICAL LABORATORIES
AIR FORCE SYSTEMS COMMAND
WRIGHT-PATTERSON AIR FORCE BASE, OHIO 45433

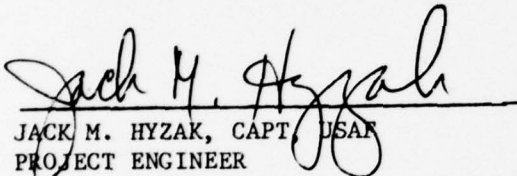
79 05 03 03 7

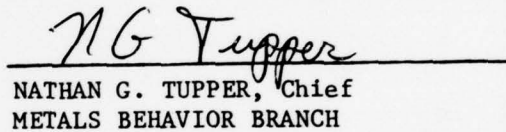
NOTICE

When Government drawings, specifications, or other data are used for any purpose other than in connection with a definitely related Government procurement operation, the United States Government thereby incurs no responsibility nor any obligation whatsoever; and the fact that the government may have formulated, furnished, or in any way supplied the said drawings, specifications, or other data, is not to be regarded by implication or otherwise as in any manner licensing the holder or any other person or corporation, or conveying any rights or permission to manufacture, use, or sell any patented invention that may in any way be related thereto.

This report has been reviewed by the Information Office (OI) and is releasable to the National Technical Information Service (NTIS). At NTIS, it will be available to the general public, including foreign nations.

This technical report has been reviewed and is approved for publication.


JACK M. HYZAK, CAPT, USAF
PROJECT ENGINEER


NATHAN G. TUPPER, Chief
METALS BEHAVIOR BRANCH

"If your address has changed, if you wish to be removed from our mailing list, or if the addressee is no longer employed by your organization please notify AFML/LLN, W-PAFB, OH 45433 to help us maintain a current mailing list".

Copies of this report should not be returned unless return is required by security considerations, contractual obligations, or notice on a specific document.

SECURITY CLASSIFICATION OF THIS PAGE (When Data Entered)

REPORT DOCUMENTATION PAGE		READ INSTRUCTIONS BEFORE COMPLETING FORM	
1. REPORT NUMBER (18) AFML-TR-78-174	2. GOVT ACCESSION NO. (19) TR-78-2747	3. RECIPIENT'S CATALOG NUMBER	
4. TITLE (and Subtitle) (6) An Analysis of the Low Cycle Fatigue Behavior of the Superalloy Rene 95 by Strainrange Partitioning	5. TYPE OF REPORT & PERIOD COVERED JAN 77 to JAN 78		
7. AUTHOR(s) (10) (a) Capt. Jack M. Hyzak (a) Henry L. Bernstein	8. CONTRACT OR GRANT NUMBER(s) (15) F33615-76-C-5191		
9. PERFORMING ORGANIZATION NAME AND ADDRESS 1) Metals Behavior Branch(LLN) 2) Systems Res. Lab. Air Force Materials Lab. Dayton, OH Wright-Patterson AFB, OH 45433 340 45440	10. PROGRAM ELEMENT, PROJECT, TASK AREA & WORK UNIT NUMBERS (16) 2307P102 (17) PY		
11. CONTROLLING OFFICE NAME AND ADDRESS 61132F	12. REPORT DATE (11) November 1978		
14. MONITORING AGENCY NAME & ADDRESS (if different from Controlling Office) Air Force Materials Laboratory (LLN) Air Force Systems Command Wright-Patterson AFB, OH 45433	13. NUMBER OF PAGES 60		
15. SECURITY CLASS. (of this report) Unclassified		15a. DECLASSIFICATION/DOWNGRADING SCHEDULE	
16. DISTRIBUTION STATEMENT (of this Report) Approved for Public Release; distribution unlimited.			
17. DISTRIBUTION STATEMENT (of the abstract entered in Block 20, if different from Report) (9) Technical rept. Jan 77-Jan 78			
18. SUPPLEMENTARY NOTES (12) 6A p.			
19. KEY WORDS (Continue on reverse side if necessary and identify by block number) Strainrange Partitioning Life Prediction Crack Initiation Rene 95 Low Cycle Fatigue			
20. ABSTRACT (Continue on reverse side if necessary and identify by block number) This report describes the results of a research program to examine the applicability of the Strainrange Partitioning (SRP) method for predicting high temperature low cycle fatigue (LCF) crack initiation. Strain controlled LCF tests were performed at 922K (1200°F) on Rene 95, a high strength nickel-base superalloy, and SRP was used to correlate the data, as well as, to predict the number of LCF cycles to failure for a series of validation tests.			

DD FORM 1 JAN 73 1473 EDITION OF 1 NOV 65 IS OBSOLETE

Unclassified
SECURITY CLASSIFICATION OF THIS PAGE (When Data Entered)

340 400

79 05 03 037

Unclassified

SECURITY CLASSIFICATION OF THIS PAGE(When Data Entered)

The data indicate that for Rene 95 compressive dwell cycles are more damaging than tensile dwell cycles, and the LCF behavior depends largely on the time in tension per cycle and on the value of the maximum tensile stress. SRP was unable to satisfactorily predict the cyclic life for several types of LCF tests because the model is not capable of accounting for particular aspects of the alloys cyclic behavior, particularly the development of mean stresses.

SECURITY CLASSIFICATION OF THIS PAGE(When Data Entered)

FOREWORD

This technical report was prepared by the Metals Behavior Branch, Metals and Ceramics Division, Air Force Materials Laboratory, Wright-Patterson Air Force Base, Ohio. The research was conducted under Project No. 2307, "Solid Mechanics", Task 2307P102, "Failure Prediction in Metals", and Air Force Materials Laboratory contract F33615-76-C-5191. This report includes work performed during the period January 1977 to January 1978. The work was performed by Capt. Jack M. Hyzak of the Air Force Materials Laboratory, and Henry L. Bernstein of Systems Research Laboratories.

The high temperature strain control testing was performed by Mar-Test, Inc. under Air Force Materials Laboratory contract F33615-76-C-5245. The authors gratefully acknowledge the valuable discussions with Messrs. Stentz, Conway, and Berling of Mar-Test, Inc. The authors also wish to thank Dr. G. R. Halford for his helpful discussions and for performing the cyclic creep tests in his laboratory. The results of the research of Dr. M. N. Menon while at the Air Force Materials Laboratory contributed to this work. The authors also wish to thank their colleagues, especially Dr. W. H. Reimann and Dr. T. Nicholas of the Air Force Materials Laboratory, and Dr. N. Ashbaugh of Systems Research Laboratories, for their assistance.

ACCESSION for	
NTIS	White Section <input checked="" type="checkbox"/>
DDC	Blue Section <input type="checkbox"/>
UNANNOUNCED	<input type="checkbox"/>
J S I CATION	
BY	
DISTRIBUTION/AVAILABILITY CODES	
SPECIAL	
A	

TABLE OF CONTENTS

Section		Page
I	INTRODUCTION	1
II	STRAINRANGE PARTITIONING - A REVIEW	3
III	EXPERIMENTAL	5
	1. MATERIALS	5
	2. TEST PROCEDURES	6
	3. DATA REDUCTION	7
IV	EXPERIMENTAL RESULTS	9
	1. BASELINE TESTS - CYCLIC RESPONSE	9
	2. STRESS BEHAVIOR	9
	3. STRAINRANGE PARTITIONING ANALYSIS	10
	a. PP LINE	10
	b. CC LINE	10
	c. PC LINE	11
	d. CP LINE	11
	4. DATA ACCEPTANCE CRITERIA	12
	5. CYCLIC CREEP TESTS	13
	6. DATA CORRELATION	15
	7. VERIFICATION TESTS	15
	a. WAVEFORMS AND PARTITIONING	16
	b. LIFE PREDICTION	17
V	DISCUSSION	18
VI	CONCLUSIONS	24
	APPENDIX I - PHASE I TEST DATA	34
	REFERENCES	36

LIST OF ILLUSTRATIONS

FIGURE		PAGE
1	Hysteresis loops for the four baseline test cycles.	38
2	Low Cycle Fatigue Data for Rene' 95 baseline strain controlled tests at 922K (1200°F). The line shown is the Manson-Coffin relationship for 30 cpm data.	39
3	Relationship of maximum tensile stress to inelastic strainrange for baseline tests. Best fit line constructed for 20 cpm data.	40
4	Relationship of mean stress.	41
5	PP life relationship for Rene' 95.	41
6	CC life relationship for Rene' 95.	42
7	PC life relationship for Rene' 95.	42
8	CP life relationship for Rene' 95 based on positive N_{CP} data only.	43
9	Semi-logarithmic plot of N_{CP} data versus $\Delta\epsilon_{in}$ in showing calculated negative N_{CP} lives.	43
10	Comparison of NASA PP data with baseline PP relationship.	44
11	Comparison of balanced cyclic creep data with the baseline CC relationship.	44
12	Comparison of compressive cyclic creep data with the baseline PC relationship.	45
13	Comparison of tensile cyclic creep data with the baseline CP relationship, and construction of the cyclic creep CP line.	45
14	Summary of partitioned strainrange-life relationships for Rene' 95.	46

LIST OF ILLUSTRATIONS (CON'D)

FIGURE		PAGE
15	Comparison of observed and predicted life for baseline tests.	47
16	Comparison of observed and predicted life for baseline tests based on cyclic creep CP line.	47
17	Illustration of intermediate strain hold cycle.	48
18	Total strain versus time waveform for fast-slow and slow-fast tests.	48
19	Comparison of observed and predicted life for validation tests based on baseline SRP relationships.	49
20	Relationships of LCF life to maximum tensile stress for baseline tests with different hold times in tension.	49
21	Relationship of maximum tensile stress with inelastic strainrange for verification tests. The line for the time independent, 20 cpm baseline tests has been included along with the critical stress limits constructed from the baseline data.	50
22	Comparison of verification test data with the maximum tensile stress-tensile hold time correlation developed for the baseline tests.	51
23	Stressrange versus total strainrange for 20 cpm and 0.05 cpm continuously cycling tests.	51

LIST OF TABLES

<u>TABLE</u>	<u>TITLE</u>	<u>PAGE</u>
I	Chemical Composition of Rene 95	25
II	Average Tensile Properties of Rene 95 at 922K	26
	Rene 95 Creep Tests at 922K	26
III	CC Partitioned Data	27
IV	PC Partitioned Data	27
V	CP Partitioned Data	28
VI	Cyclic Creep Tests - Partitioned Data	28
VII	Baseline Data Correlation	29
VIII	Unbalanced Strain Hold Tests - Partitioned Data	30
IX	Intermediate Strain Hold Tests - Partitioned Data	31
X	Low Rate Strain Cycle Tests (.05 CPM) - Partitioned Data	31
XI	Variable Rate Straincycle - Partitioned Data	32
XII	Verification Tests - SRP Life Prediction	32
XIII	Life Prediction - Validation Tests - Stress/Time Equations	33

SECTION I

INTRODUCTION

A major area of concern in the development of recent military turbine engines has been life cycle management. A part of the technology needed to optimize the life of components, such as turbine disks, is the ability to accurately predict their crack initiation lives under typical cyclic conditions. With the increasing turbine temperatures that accompany performance gains, the turbine section operating conditions are becoming increasingly severe. Typical military flight missions include significant dwell periods at high power settings with the result that time dependent damage mechanisms operate. This has necessitated modification of existing life relationships previously relied upon at lower temperature.¹ One such development has been the Strainrange Partitioning^{1,2,3} (SRP) method for predicting creep-fatigue interactions.

It has been shown in the literature that SRP can be a valuable tool in analyzing creep-fatigue interactions in many alloys.^{3,4,5} In one summary⁶, data for twelve different alloys were analyzed, and SRP was successful in correlating lives within a factor of two. The alloys that have been studied are, however, generally more ductile than the high strength nickel-base superalloys. Time dependent deformation constitutes a large fraction of the total inelastic strains in these more ductile alloys, and research has been concentrated in the cyclic life range where inelastic strains are also comparatively large. At these levels of inelasticity, the stress response of the alloys is generally more predictable than at lower strain ranges, in particular, significant mean stresses do not usually develop.

Menon⁷ has reported that, for the superalloy Rene' 95, stress relaxation during strain hold cycles is rather limited at 922K (1200°F) and the fractions of time dependent strain are small. This behavior is particularly marked approaching the life range of interest for practical engineering design (5,000 - 50,000 cycles). Although the "creep" strains are small,

the response of Rene' 95 to strain hold cycles is rather pronounced. This paper will describe the reaction of Rene' 95 to strain controlled fatigue at 922K and discuss the influence of various test parameters on the fatigue behavior. The high temperature LCF data will be analyzed using SRP and an evaluation will be made of how effective the model is in correlating the data base, as well as predicting crack initiation lives for different test conditions. This research was performed at the Air Force Materials Laboratory.

SECTION II
STRAINRANGE PARTITIONING - A REVIEW

The basic premise of the Strainrange Partitioning Method for predicting LCF crack initiation is that the creep-fatigue life is controlled primarily by the ability of a material to absorb cyclic inelastic strain. Two inelastic strain components are recognized by the method: "creep", associated with thermally activated, time dependent deformation, and "plasticity", associated with time independent deformation. An important feature of the method is that it draws a further distinction between the manner in which tensile inelastic strain is reversed by the compressive inelastic strain to establish a closed hysteresis loop. The four generic types of strain cycles are therefore:

$\Delta\epsilon_{PP}$: tensile plastic flow reversed by compressive plastic flow

$\Delta\epsilon_{CC}$: tensile creep reversed by compressive creep

$\Delta\epsilon_{PC}$: tensile plastic flow reversed by compressive creep

$\Delta\epsilon_{CP}$: tensile creep reversed by compressive plastic flow

Life relationships similar to the Manson-Coffin relationship are established for each of the four types of strain loops by performing completely reversed strain-cycling fatigue tests. Once these relationships have been established, the cyclic life for any high temperature cycle involving completely reversed strains can be calculated using the interaction damage rule.⁶ The interaction damage rule is expressed by the equation:

$$\frac{1}{Nf} = f_{PP}/N_{PP} + f_{PC}/N_{PC} + f_{CP}/N_{CP} + f_{CC}/N_{CC} \quad (1)$$

where: N_f = cyclic life under some complex hysteresis loop

f_{ij} = constitutive fraction of type i,j inelastic strain

N_{ij} = cyclic life expected where entire inelastic strain is
of type ϵ_{ij}

It should also be noted that pure PC, CP, and CC tests cannot be experimentally generated because there is always some PP strain component present. Therefore, in developing the four basic SRP life relationships from the LCF test results, the interaction damage rule must be used to partition the amount of fatigue damage that is to be attributed to each type of strain.

SECTION III EXPERIMENTAL

1. MATERIALS

Rene' 95 is a high strength, nickel-base superalloy primarily used for turbine disks in recent turbine engines. The alloy composition is given in Table I. In addition to the conventional strengthening mechanisms involving precipitation of a high volume fraction of gamma prime, and to a lesser degree solid solution hardening, Rene' 95 derives part of its strength from the residual dislocation substructure introduced during a thermomechanical processing treatment (TMP). TMP is also responsible for the duplex structure of Rene' 95, often called the "necklace structure", in which large warm worked grains (75 μ m) are surrounded by a necklace of fine recrystallized grains (4 μ m). The result of TMP and conventional hardening treatments is an improvement in tensile and rupture strength at temperatures to about 922K.

The two pancakes of Rene' 95 used in this program were taken from a vacuum induction melted and vacuum arc remelted ingot approximately 0.228m in diameter. The ingot was given a homogenization anneal in the range 1263K - 1436K for 3 hours and then furnace cooled. The pancakes were subsequently reheated to 1366K - 1410K and forged to bring the thickness to 40-50% above the final value. This was followed by a recrystallization anneal at 1436K for one hour. This results in a uniform grain diameter between .064 - .127mm. The forgings were cooled from the recrystallization temperatures at a rate greater than 93.3K per hour to 1172K and then air cooled and taken to final processing. The forgings were reheated to 1352K - 1380K and the final reduction was applied, resulting in a further 40-50% decrease in thickness. The pancakes were then partially solutioned at 1366K, oil quenched to a temperature below 755K, and aged at 1035K for 16 hours.

The Rene' 95 forgings have been characterized in terms of microstructure⁸, tensile behavior⁹, and room temperature LCF crack initiation mechanisms.¹⁰ The tensile and creep properties of Rene' 95 are summarized in Table III.

2. TEST PROCEDURES

The low cycle fatigue tests were performed using a servohydraulic closed loop system. The test specimens were of the standard hourglass design with a 6.35mm (.250 inch) minimum diameter. A diametral extensometer along with a strain computer was used to monitor and control the tests.¹¹ All tests were conducted at 922K (1200°F). Test cycles were completely reversed, zero mean strain. Specimens were heated using an induction system with control thermocouples attached in the radius section away from the minimum diameter.

The test plan consisted of three phases: baseline testing under strain control, cyclic creep tests utilizing load control to strain limits, and validation testing comprised of less conventional waveforms. The Phase I, baseline test procedures, will be discussed here. The cyclic creep tests and validation testing will be described in separate sections.

The baseline testing was designed to evaluate the LCF properties of Rene' 95 at 922K and to provide sufficient data with which to establish the SRP life relations under PP, PC, CP, and CC loading. The test matrix was comprised of high rate strain cycles, as well as tension, compression, and balanced strain hold tests. Figure 1 shows hysteresis loops for the four types of tests.

The continuous cycling tests were diametrically monitored and the total axial strain was controlled. The specimens were tested at 20 cycles per minute (.333 Hz) using a triangular waveform. This frequency represents the upper limit of the test system and is at a high enough rate to preclude time dependent deformation in Rene' 95 at 922K at the strain ranges tested.

The dwell cycles incorporated hold times in tension, compression, and both (balanced strain hold cycles). These tests were also strain controlled. The ramp rate was the same as for a 20 cycles per minute (cpm) test. The strain limit was maintained during the dwell and the load was allowed

to relax. Both one and ten minute hold times were used. These tests will be denoted as (X/Y) tests where X is the number of minutes held in tension and Y is the time held in compression, i.e., a one minute tensile hold test is designated as (1/0).

3. DATA REDUCTION

The SRP life relationships have been derived using the interaction damage rule. The strain ranges were partitioned from the load and inelastic strain stripchart recordings. For the strain hold cycles, the creep strain was defined as the inelastic strain that developed during stress relaxation. The value was calculated by dividing the decrease in stress during the hold period by the elastic modulus.³

Because Rene' 95 cyclically softens at 922K, there was generally a significant increase in the inelastic strain throughout a test. For the 20 cpm tests, the inelastic strainrange increased between 13% and 130% of the original value. The amount of softening generally increased as the total strainrange decreased. The reported values of load and strain are the values at half-life ($N_f/2$). These values were used in the SRP analysis.

All cyclic life values are cycles to failure (N_f). Several methods, however, were examined to establish a value of cycles to crack initiation (N_i). The most sensitive criterion was to visually determine the point at which the slope of the relationship of the maximum tensile stress with time changed. This point was then designated the time of crack initiation. For the baseline strain controlled tests the earliest indication of initiation using this criterion was 85% of the cycles to failure. Most values, however, were greater than 90% N_f .

The data were also analyzed using the 5% and 10% load drop criteria. Initiation was defined as the point at which the maximum tensile load decreased the designated percentage from the cyclic softening load line.

These values of N_i were necessarily even higher fractions of the total life than for the previously discussed criterion. In light of these results, it was concluded that no significant benefit would be realized by using some measure of N_i rather than N_f .

For the SRP analysis, the best fit life relationships of the form

$$\Delta\epsilon_{in} = C N_{ij}^B \quad (2)$$

C, B constants

have been determined. A least squares fit to the data was obtained in the sense that the sum of the squares of the error

$$\log N_{ij}^{\text{PRED}} - \log N_{ij}^{\text{OBS}} = \frac{1}{B} \{ \log(\Delta\epsilon_{in}) - \log C \} - \log N_{ij}^{\text{OBS}} \quad (3)$$

was a minimum.

SECTION IV

EXPERIMENTAL RESULTS

1. BASELINE TESTS - CYCLIC RESPONSE

As has been mentioned, Rene' 95 is a relatively creep resistant alloy at 922 K. The reaction of the material to strain hold cycles, however, is significant. Results are presented in Fig. 2 for the various hold tests along with the high rate strain cycle tests performed at 20 cpm. Inelastic strainrange is plotted versus cycles to failure, and the best fit line is drawn through the 20 cpm test points. This is the Manson-Coffin relationship for time independent behavior. These data indicate that at the same inelastic strain compressive hold tests are the most damaging, while the tension strain hold tests produce longer lives than the creep free high rate strain tests. The latter result is particularly pronounced at the lower inelastic strain ranges. Fig. 2 further shows that the use of the Manson-Coffin relationship would result in a potential error of a factor of five in predicting the data.

2. STRESS BEHAVIOR

The material response of Rene' 95 is such that large shifts develop in the maximum tensile stress during some strain hold cycles as compared to the 20 cpm, time independent, behavior. These changes are in addition to the reductions in stressrange that accompany cyclic softening. A plot of the maximum tensile stress versus inelastic strainrange is shown in Fig. 3. These data are for the baseline strain controlled tests. Compressive hold tests develop significantly higher peak tensile stresses at a given inelastic strainrange than do the 20 cpm tests, and the tensile and balanced strain hold tests have lower tensile stresses than the 20 cpm tests. The shift in peak tensile stress for these data increases as the strainrange is reduced and the hold time lengthened. This behavior is generally

reflected in the value of the mean stress. Fig. 4 shows the mean stress as a function of inelastic strainrange for these same tests. Compressive hold tests develop a positive mean stress while the continuously cycling tests and tension and balanced hold cycles have negative mean stress values. As with the tensile stress data, Fig. 3, the largest biases develop in the tensile strain hold tests at the lower strainranges and longer hold times.

3. STRAINRANGE PARTITIONING ANALYSIS (PHASE I)

The high rate strain cycle tests and the strain hold cycle tests comprised the baseline testing program. These data were used to construct the four SRP life relations from which validation tests were predicted. All baseline test data are listed in Table I of the Appendix.

a. PP Line

The high rate strain cycle tests (20 cpm) contained only plastic inelastic strains. They, therefore, formed the basis of the PP relationship. The data are shown in Fig. 5. The best fit power law equation for the PP line is:

$$\Delta\epsilon_{PP} = 0.736 (N_{PP})^{-0.896} \quad (4)$$

b. CC Line

Balanced strain hold tests were performed to generate CC data. These were both 1/1 hold (one minute hold in tension and one minute hold in compression) and 10/10 hold tests. Due to the differing stress relaxation response of the alloy in tension and compression, the tests in most cases contained small amounts of PC or CP strain. The partitioned strains, cycles to failure, and the calculated values of life and percent damage are listed in Table III. The percent damage attributed to a particular strain component is calculated using the equation⁶:

$$\frac{f_{ij}}{N_{ij}} N_f (100) = \% \text{ damage} \quad (5)$$

The calculated CC data points are shown in Fig. 6. The equation of the CC line is:

$$\Delta\epsilon_{PC} = 0.198 (N_{PC})^{-0.852} \quad (6)$$

c. PC Line

The PC damage was partitioned from compressive strain hold tests. The hold periods were for one and ten minutes. The partitioned data are presented in Table IV. The PC points and line are shown in Fig. F. The equation of the PC line is:

$$\Delta\epsilon_{PC} = 0.135 (N_{PC})^{-0.914} \quad (7)$$

d. CP Line

The CP points were calculated from 1/0 and 10/0 tension hold strain data. These cycles have been previously shown to be less damaging than high rate strain cycles when compared at the same inelastic strain ranges (Fig. 2). Because tension hold cycles are significantly less damaging than PP cycles at lower strain levels, the values of N_{CP} calculated from the interaction damage rule are negative. These calculations suggest that not only is CP strain in this range less damaging than PP, but it can be considered "rejuvenating" when incorporated with PP damage. This is emphasized by considering that for those tests with a negative N_{CP} life, N_f was significantly greater than the life predicted for the partitioned $\Delta\epsilon_{pp}$ component alone.

The CP data are presented in Fig. 8 and Table V. The points with negative calculated N_{CP} lives are plotted at the appropriate strain levels. These data are also plotted on a less conventional semi-logarithmic plot (Fig. 9) in order to present the negative life values and to show the discontinuous nature of the function.

Because the present formulation of SRP does not provide a basis for describing negative life behavior, certain approximations will be made in order to continue the analysis. There seems to be no straightforward method for developing a single life relationship using both the positive and negative N_{CP} points. The graphical construction of a relationship representing all tests is unclear since it appears from Figs. 8 and 9 that the value of strain at which the N_{CP} lives change from positive to negative values depends on the hold time of the cycle. Therefore, a single CP life relationship has been established on the basis of only those data points with positive N_{CP} lives. This relationship will be conservative in predicting the negative N_{CP} lives.

The equation of the line through the positive N_{CP} points is:

$$\Delta\epsilon_{CP} = 2.20 (N_{CP})^{-1.217} \quad (8)$$

This relationship was used in the calculation of the CP damage in the balanced strain hold tests.

4. DATA ACCEPTANCE CRITERIA

In order to establish a valid SRP life relationship, it is essential that a significant portion of the damage in a baseline test be due to the strain component of interest. A criterion has been proposed to determine if a test point meets this requirement.⁶ This standard requires that the percent damage, defined by Eq. (5), attributed to the strain component of interest be greater than 50%, and it further states that the fraction of creep strain (f_{CC} , f_{CP} , f_{PC}) in the test should be greater than one-half.

This validity criterion has not been applied to the data. Although the intent of the standard is appreciated, it appears that in this case

it would unfairly bias the life relationships. In general, the CC and PC data points do have calculated values of percent damage greater than the required 50%. Several points that do not meet this criterion, however, have also been included. The reason for this is that points that last longer than predicted by the best fit lines have calculated values of percent damage less than points that scatter even farther from the line but into the lower life range. Also, for much of the data, the calculated values of percent damage did not change predictably with changes in the fraction of creep strain. A more consistent correlation would be expected if the percent damage was a good measure of the cyclic life expended due to creep. Therefore, omitting the points with less than 50% creep damage would in this case prejudicially bias the life lines toward the lower life range.

The CP points, in general, did not meet the percent damage criterion. However, because of the unusual results from applying the interaction damage rule to these data and because there was not a good correlation between percent damage and f_{CP} , the CP points were considered valid.

Although not strictly required by the criterion, the fractions of creep strain for the baseline tests were not greater than one-half. These small creep strains are a result of the type of test cycle employed. Because there is stress relaxation in a strain hold cycle and due to the limited creep response of Rene' 95 at 922K, the fractions of CC, CP, and PC damage in all baseline tests were small. The response of the material of these small creep strains, however, was significant with the result that most tests did meet the 50% damage criterion as required. The baseline test data were therefore considered valid points with which to establish the SRP life relationships.

5. CYCLIC CREEP TESTS (PHASE II)

In the strain hold cycle baseline testing previously reported, the strain component of interest (PC, CP, CC) comprised only 10-35% of the

total inelastic strainrange. To corroborate the validity of these data, several cyclic creep tests were performed at the NASA-Lewis laboratory. In these tests, the load was ramped to a prescribed value and was then held constant. The specimen was then allowed to creep to a set diametral strain limit at which time the load was reversed. These tests were successful in generating approximately 50% of the total inelastic strain as creep strain.

Due to the cyclically softening behavior of Rene' 95, cyclic creep tests need to be continually monitored. Adjustments must be made in the load level and strainrange in order to maintain the same proportions of each strain component while still limiting the tests to a reasonable cyclic period. The strain fractions, therefore, necessarily varied, and the reported values are the best estimate for each test.

It should also be noted that as a result of these tests being performed in a different laboratory, the specimen geometry and orientation were not the same as used for the baseline and validation testing. The purpose of presenting these data then is to see if incorporating larger percentages of creep damage in a test grossly alters the life relationship developed from the strain hold testing.

The results of the cyclic creep tests are presented in Table VI and Figs. 10-13. Two additional PP type tests were also performed and data points are plotted in Fig. 10. These points are consistent with the baseline PP data. Due to the limited number of data points, however, the original baseline PP relationship was used to partition the cyclic creep tests. The CC and PC points are shown in Figs. 11 and 12. They, too, are in good agreement with the strain hold data.

The relation of the cyclic creep CP points to the CP strain hold data is less obvious due to the large amount of scatter in the data (Fig. 13). Because of the potential error in characterizing the strain fractions of the cyclic creep tests and due to the limited strain range tested, these two points can be considered in the general scatter band of the

strain hold points. However, in light of the overall uncertainty in defining the response of Rene' 95 to CP damage and in an attempt to be thorough in this analysis, a second CP line has been constructed as a best fit through the two cyclic creep points and baseline tests #10 and #228. The choice of the two strain hold data points (#10, #228) is based on the fact that these two tests do contain the required 50% CP damage. This CP line is defined by the equation:

$$\Delta\epsilon_{CP} = .056 (N_{CP})^{-0.689} \quad (9)$$

and will be referred to as the cyclic creep CP line. A summary of the SRP relationship for Rene 95 is presented in Fig. 14.

6. DATA CORRELATION

Based on the four SRP life relationships developed from the Phase I baseline data, the expected lives for those same tests were predicted using the interaction damage rule. The predicted values (N_{PRED}) are compared with the actual lives (N_f) in Table VII and Fig. 15. The majority of data lie within a factor of two from the predicted lives. Five test points, however, lie outside this range. Three tensile hold tests are underpredicted while one compressive hold test and one 20 cpm test are non-conservatively predicted. The largest deviation is a factor of 5.5 for a low strainrange tensile hold test.

Similar results are presented in Fig. 16 for the lives predicted using the cyclic creep CP line. In this case, five tensile hold tests are underpredicted by more than a factor of two, and still the compressive hold test and the 20 cpm test are predicted nonconservatively.

7. VERIFICATION TESTS - PHASE III

In order to truly test the predictability of SRP, several additional tests were performed and their lives predicted on the basis of the SRP life relations previously presented. The waveforms for these tests were generally of a different character than utilized in the baseline testing.

These include unbalanced strain hold tests, intermediate strain hold tests, 0.05 cpm slow rate strain cycles, and fast-slow and slow-fast strain cycles.

a. Waveforms and Partitioning

The unbalanced strain hold cycles consisted of strain hold times of differing durations in tension and compression. This cycle was an attempt to incorporate significant amounts of three types of strain in one test. Both 10/1 and 1/10 cycles were tested. The creep strains were partitioned from the stress relaxation curves. Test conditions and partitioned strain values are presented in Table VIII.

The intermediate strain hold cycle was conceived of as a means of altering the sequence of inducing time dependent and time independent strains. The strain hold was introduced at a total strain value less than the total strain limit (Fig. 17). Thus, the specimen was strained to a set value and maintained for a period at that strain level while the load relaxed. The specimen was then strained in the same loading direction to a final strain limit. Test conditions included one minute intermediate holds in either tension or compression (11/0, 0/11). The creep strains again were partitioned from the relaxation records. The data are presented in Table IX.

The third type of validation test was the 0.05 cpm continuously cycling low rate strain cycle. Six tests were performed. Five of the tests were run under inelastic strain control; test 34 was tested under total strain control as were the baseline tests. Only three of the six tests were partitioned. The test conditions and the partitioned data for all 0.05 cpm tests are presented in Table X.

To partition the strains for the 0.05 cpm tests, the rapid load method was used on a companion specimen.¹² The companion test was first cycled at the appropriate strain level at 0.05 cpm under strain control. The test was then changed to load control and the load limits previously established in the 0.05 cpm testing were imposed. The specimen was

then cycled under these conditions at 20 cpm. The difference in the inelastic strain ranges at the two frequencies (0.05 and 20 cpm) was then considered to be the creep component. The fractions of inelastic strain (f_{CC} , f_{PP}) were assumed to be the same for the actual 0.05 cpm test. As shown in Table X the fractions of creep strain in these tests approached zero.

The fourth type of verification test was the variable rate strain test involving fast-slow and slow-fast cycles. A fast-slow cycle consists of ramping from the minimum strain to the maximum strain in 1.5 seconds (20 cpm rate) and then ramping from the maximum strain back to the minimum strain in 600 seconds (0.05 cpm rate). A slow-fast cycle involves just the opposite sequence. Both test cycles are illustrated in Fig. 18. The rapid load method was used to partition the tests. The fraction of creep strain (f_{CC}) for both tests was 0.12. The results are presented in Table XI.

b. Life Prediction

The predicted fatigue lives for the verification tests were calculated from the partitioned data using the interaction damage rule and the SRP life relations previously established in Phase I. The expected values are compared with the observed lives in Fig. 19 and Table XII.

SRP predicts both the unbalanced strain hold tests and the intermediate strain hold tests very accurately. The largest variation from the predicted life was a factor of 1.64. Both the 0.05 cpm tests and the variable rate tests, however, were not generally predicted within a factor of two. Two of the tests varied by a factor of 2.4 and the one slow-fast rate test was non-conservatively predicted by greater than an order of magnitude.

SECTION V

DISCUSSION

These data have shown that SRP can be used to predict crack initiation life for Rene 95 under certain test conditions. The majority of the baseline tests, particularly at the larger strain ranges, were effectively correlated using SRP, and all the strain hold verification tests were predicted within a factor of 2. Other test cycles, however, were not as accurately modeled. Several baseline tensile strain hold tests and one compressive hold test were not predicted by SRP within a factor of 2. The low rate continuously cycling tests were also poorly predicted. In addition, it has been noted that the results of the partitioned CP data do not appear consistent with the basis of SRP. In general then, the results of this research indicate that there are fundamental limitations in applying SRP in its present form to this type of alloy.

Of particular concern is the fact that a meaningful life relationship could not be established for CP damage in the longer life region. In the SRP analysis (Sect. IV, 3.), baseline tensile strain hold tests were partitioned and the N_{CP} lives were calculated using the interaction damage rule. As previously noted, the calculated values of N_{CP} for several of the low strain range tests were negative. This is a result of the fact that at low strain levels tensile strain hold cycles are considerably less damaging than high rate strain cycles. The interaction damage rule, as presently conceived, does not account for this behavior. This is because the rule can be considered asymptotic in nature.¹³ Thus, even for the hypothetical case where the other contributing lives were infinite, the maximum value possible for life computed using the rule equals the shortest contributing life (PP, PC, CP, or CC) times the inverse of its constitutive fraction.

There is, however, a more general inconsistency between the data and SRP. The results indicate that there is a direct and significant influence of the maximum tensile stress on fatigue life which is not accounted for by SRP. As has been described, stress shifts usually develop during strain hold testing. The value of the maximum tensile stress increases during

a compressive hold test and decreases during tensile and balanced hold tests. For these data, the change in the value of the peak tensile stress compared to the 20 cpm continuously cycling behavior has been shown to increase as the inelastic strainrange decreased and the hold time increased (Fig. 3). These results correlate with the trends observed in life (Fig. 2). Compressive hold tests consistently have shorter fatigue lives than tensile hold cycles for the same inelastic strainranges, and the differences in life are greatest at the lower strainranges and for longer hold times. Similar behavior has been reported for the high strength, low ductility alloy IN 738¹⁴, Rene 80¹⁵, and for the relatively ductile CR-Mo-V steel when tested at lower strainranges.¹⁶

The strainhold baseline data have been plotted on semi-log axes to directly show the dependence of life on peak tensile stress, σ_{tmax} (Fig. 20). This type of analysis has been suggested by Conway^{17, 18} for creep data. The data fall generally onto three straight lines. The fast rate strain data and the compressive strain hold data fall on one line, the 1/0 and 1/1 strain hold points fall on the second line, and finally the 10/0 and 10/10 data can be fit with a third line. Each line corresponds to a particular tensile hold time, t_t (0, 1, 10 minutes). Linearity on semi-log axes indicates an exponential relationship between maximum σ_{tmax} and N_f . The best fit lines are drawn through the appropriate data in each case. The values of N_f compare with the lives predicted from these lines within a factor of two except for one 0/1 test (#11). These relationships illustrate the influence of peak tensile stress and tension hold time on fatigue life. They are not, however, proposed as a predictive model.

In light of these findings, the results of the baseline data correlation (Sect. 3.6) can be more easily understood. Five baseline tests were not correlated by SRP within a factor of two (Fig. 15). The one PP test (#29) should be considered a statistical anomaly since it does not correlate well with the other data. The other four tests (#222, 233, 33, 237), however, are strain hold tests which display a consistent behavior. The three tensile hold tests developed the largest maximum tensile stress

biases of the tensile hold baseline tests, while test #222 developed the largest tensile stress bias of the compressive hold tests (Fig. 2). The stress bias for this analysis is defined to be the difference between the value of the maximum tensile stress for the particular test and the value of the peak tensile stress for a PP test at the same inelastic strainrange. The PP data is defined by the best fit line through the 20 cpm tests (Fig. 3).

These results further highlight the influence of peak tensile stress on fatigue life, and they suggest that when the stress bias is greater than some critical value, SRP does not accurately predict life (within a factor of 2). Consistent with these results is the behavior of the balanced hold tests. These tests do not develop as severe a reduction in the peak tensile stress as do the tensile hold tests. The balanced strain hold tests would, therefore, not be expected to fall outside the range of predictability by SRP, as is observed.

The results of the verification tests, however, cannot be totally explained in terms of the stress bias. The maximum tensile stress for each of the verification tests is plotted versus inelastic strainrange in Fig. 21 along with the $\Delta\epsilon_{in}$ versus maximum σ_t relationship for the 20 cpm tests previously displayed in Fig. 3. The critical stress bias limits have also been constructed from Fig. 3. These limits represent the boundaries between satisfactorily correlated baseline tests and those not correlated within a factor of two. The maximum tensile stress values for the unbalanced and intermediate strain hold tests all lie within the stress bias limits. The actual fatigue lives for these tests were predicted by SRP within a factor of 2. The two 0.05 cpm tests that were not accurately predicted by SRP, however, do not have peak tensile stresses greater than the critical values, and the fast-slow test was predicted by SRP in spite of falling outside the critical stress units. These results suggest that for strain hold tests the peak tensile stress is a controlling parameter, but for low rate continuously cycling tests there is a more dominant factor.

The lives of the verification tests were also compared to the lives that would be expected on the basis of the peak tensile stress-tensile hold time correlation described by Fig. 20. For this analysis, the tension going time per cycle for the continuously cycling tests was used in place of the hold time in tension. Thus, the 0.05 cpm tests were compared to the 10 minute tensile hold data as was the slow-fast test, and the fast-slow test was compared to the zero hold time data. The intermediate tensile hold tests were also compared to the zero tensile hold time relationship since the tensile hold period for these tests was at a stress level less than the maximum stress. The data are presented in Fig. 22 and Table XIII.

All the verification tests agreed with the tensile stress-time lines within a factor of 1.85 which further indicates that the high temperature, low cycle fatigue behavior of Rene'95 is dependent on the value of the maximum tensile stress and some measure of the cycle time in tension. It appears then from these results that SRP is unable to accurately predict certain tests because a totally strain based model, such as SRP, cannot in all cases account for changes in stress and waveshape which have been shown to significantly influence the life of Rene'95.

The fact that the 0.05 cpm verification tests were correlated using a factor for the tension going time may be the basis for explaining their behavior. The 0.05 cpm verification tests generally failed in one-half the cycles expected for 20 cpm tests at the same inelastic strainranges. As previously reported, however, the 0.05 cpm tests contained negligible partitioned creep strains. The results of the partitioning are supported by comparing the total stressranges and strainranges for the 0.05 cpm and 20 cpm tests (Fig. 23). Figure 23 shows that both 0.05 cpm and 20 cpm cycles generated approximately equal stressranges when tested at the same total strainrange. A reduction in stressrange would have been expected if time dependent creep deformation was present in the 0.05 cpm tests. These results indicate that although the time in tension per cycle is a controlling parameter, creep damage is not responsible for reducing the life of the 0.05 cpm tests. As previously stated, SRP in its present form cannot account for reductions in fatigue life not associated with a change in inelastic strains. This

also suggests that environmental factors may be governing crack initiation for low rate continuously cycling tests.

Other models^{19,20,21} have been suggested which directly account for the influence of time and peak tensile stress. Ostegren¹⁴, in particular, has proposed a model which includes terms for frequency and the product of the maximum tensile stress and inelastic strainrange. These models have not been critically examined with respect to these data and will not be treated in this analysis.

Only limited metallurgical studies have been performed on the fracture surfaces of the Rene'95 specimens to date. Additional electron microscopy and metallographic sectioning studies are required to identify initiation mechanisms, as well as crack propagation modes. Work also needs to be concentrated on examining the basic response of Rene'95 under different cyclic conditions. Strainrate effects, and cyclic softening and aging phenomena, need to be better understood. For example, the response of Rene'95 to the 0.05 cpm cycle and the variable rate verification cycles need to be more thoroughly studied in order to identify the failure controlling mechanisms.

It has been proposed²² that the advantage of SRP and the interaction damage rule is that data can be generated in the relatively low life region to develop functional life relations, and predictions can then be extrapolated into the longer life range. This research has shown that this is not the case for Rene'95. Predictions of long life compressive hold and low rate strain cycle tests could be dangerously nonconservative using this approach.

References have previously been made to alloys that behave similarly to Rene'95. On-going research at this laboratory indicates that the high strength nickel-base super-alloy, AF2-1DA, also develops a large peak tensile stress shift during strain cycling. It is also possible that other more ductile alloys may develop similar stress biases when fatigued at very low inelastic strainranges.

As previously described, SRP was able to accurately predict crack initiation in Rene' 95 for certain test conditions. For the strain hold tests, SRP was effective when the inelastic strainrange was relatively large and the hold time was short. In the range of more practical design interest, however, SRP did not consistently predict the data within a factor of two. This result has been related to the development of increasingly large biases in the value of the peak tensile stress produced at lower strainranges and with increasing hold times.

For the low rate continuously cycling tests, the applicability of SRP is not as clearly defined. SRP was not able to accurately predict lives even for high strainrange, low life tests. Additional testing and analysis is needed to further understand this behavior.

SECTION VI

CONCLUSIONS

- 1) Strain hold tests on Rene' 95 have shown that compressive hold cycles are more damaging than tensile hold cycles when the two are compared at the same inelastic strainrange. This can be explained by the fact that compressive hold cycles develop larger peak tensile stresses than do tensile hold cycles.
- 2) Strainrange partitioning was able to correlate the baseline data and predict validation tests for a limited range of conditions. SRP could not accurately predict crack initiation life for low frequency continuously cycling tests, or for strain dwell tests in the larger life region where mean stresses developed.
- 3) Maximum tensile stress and time in tension per cycle have been shown to significantly influence the crack initiation life of Rene' 95. Strainrange Partitioning cannot in all cases account for these parameters since SRP is a totally strain based model.
- 4) SRP, in its present form, does not appear applicable for predicting the crack initiation of high strength nickel-base superalloys at the relatively small inelastic strainranges of interest.

TABLE I
CHEMICAL COMPOSITION OF RENE 95

Nickel	61%*
Chromium	14%
Cobalt	8%
Tungsten	3.6%
Aluminum	3.6%
Molybdenum	3.5%
Niobium	3.5%
Titanium	2.5%
Carbon	0.15%
Iron	0.13%
Silicon	<0.10%
Manganese	<0.10%
Zirconium	0.04%
Boron	0.012%
Phosphorous	<0.01%
Nitrogen	0.003%
Sulfur	0.002%
Lead	<0.001%
Oxygen	7 ppm
Silver	<5 ppm
Bismuth	<1 ppm

*WT %

TABLE II

AVERAGE TENSILE PROPERTIES OF RENE 95 AT 922K

Yield Stress:	175 ksi
Ultimate Stress:	210 ksi
Modulus of Elasticity:	25.4×10^3 ksi
% Reduction in Area:	12%
% Elongation:	11%

RENE 95 CREEP TESTS AT 922K

Specimen	Stress (ksi)	Secondary Creep Rate (in./in./min.)	Time to Failure (min.)
C-1-B	180	5.26×10^{-4}	94
C-2-B	171	4.85×10^{-5}	433
C-4	171	6.90×10^{-5}	430
219	160	4.00×10^{-5}	960

TABLE III
CC PARTITIONED DATA

SPEC	ϵ_{in}^1	ϵ_{PP}^1	ϵ_{CC}^1	ϵ_{PC}^1	ϵ_{CP}^1	f_{CC}	% DAMAGE	N_{CC}
1	.550	.437	.085	.000	.028	.15	42	57
2	.349	.276	.055	.000	.018	.16	46	81
32	.201	.163	.028	.000	.010	.14	54	92
9	.122	.087	.030	.005	.000	.25	23	1021
15	.078	.054	.020	.000	.004	.26	47	696
28	.701	.486	.188	.000	.027	.27	52	59
31	.497	.304	.170	.000	.023	.34	48	142
230	.175	.104	.060	.000	.011	.34	71	160

1) PERCENT STRAIN

TABLE IV
PC PARTITIONED DATA

SPEC	ϵ_{in}^1	ϵ_{PP}^1	ϵ_{PC}^1	f_{PC}	% DAMAGE	N_{PC}
6	.429	.370	.059	.14	43	67
11	.468	.406	.062	.13	36	77
14	.324	.282	.042	.13	55	51
8	.192	.168	.024	.13	53	98
13	.098	.089	.009	.09	52	146
241	.049	.044	.006	.11	51	428
16	.010	*	----	---	--	---
238	.028	.023	.006	.20	43	2095
222	.136	.116	.020	.15	83	40
41	.185	.130	.055	.30	75	112

1) PERCENT STRAIN

* COULD NOT ACCURATELY PARTITION

TABLE V
CP PARTITIONED DATA

SPEC	ϵ_{in}^1	ϵ_{PP}^1	ϵ_{CP}^1	f_{CP}	% DAMAGE	N_{CP}
245	.657	.539	.118	.18	28	112
5	.522	.447	.075	.14	13	288
10	.297	.262	.035	.12	52	59
7	.206	.175	.031	.15	10	1125
12	.089	.083	.006	.07	33	274
39	.089	.070	.019	.21	22	1710
38	.049	.043	.006	.12	--	-2214
233	.061	.053	.008	.12	--	-762
33	.038	.036	.002	.05	--	-530
237	.046	.041	.005	.10	--	-578
228	.180	.150	.030	.17	51	156
40	.126	.102	.024	.19	--	-2510

1) PERCENT STRAIN

TABLE VI
CYCLIC CREEP TESTS - PARTITIONED DATA

SPEC	TYPE/ ϵ_{ij}	$\Delta\epsilon_{in}^1$	f_{PP}	f_{CC}	f_{CP}	f_{PC}	N_{ij}	N_f
RE-11	HRSC/PP	1.24	1.00	.000	.000	.000	72	72
RE-16	HRSC/PP	.308	1.00	.000	.000	.000	671	671
RE-20	TCCR/CP	.777	.529	.000	.471	.000	18	34
RE-14	TCCR/CP	.306	.530	.000	.470	.000	68	124
RE-4	CCCR/PC	.810	.498	.000	.000	.502	15	27
RE-15	CCCR/PC	.125	.610	.000	.000	.390	228	454
RE-7	BCCR/CC	.930	.342	.603	.055	.000	27	39
RE-13	BCCR/CC	.304	.345	.517	.138	.000	109	164
RE-10	BCCR/CC	.146	.611	.389	.000	.000	202	398

TABLE VII
BASELINE DATA CORRELATION

SPEC	TYPE	N_f	N_{PRED}	N_f/N_{PRED}	N_{PRED}^*	N_f/N_{PRED}^*
21	20 cpm	203	158	1.28		
17	20 cpm	234	247	0.95		
18	20 cpm	307	350	0.93		
224	20 cpm	415	569	0.73		
22	20 cpm	461	446	1.03		
240	20 cpm	463	492	0.94		
26	20 cpm	784	667	1.18		
27	20 cpm	1629	1508	1.08		
29	20 cpm	5158	10792	0.48		
30	20 cpm	16215	17263	0.94		
234	20 cpm	19160	15209	1.26		
235	20 cpm	22364	24390	0.92		
239	20 cpm	28697	15209	1.89		
245	1/0	171	174	0.98	82	2.09
5	1/0	255	226	1.13	126	2.02
10	1/0	257	417	0.62	282	0.91
7	1/0	748	591	1.27	408	1.83
12	1/0	1289	1579	0.82	1450	0.89
39	1/0	1781	1274	1.40	1049	1.70
38	1/0	5013	2716	1.85	2668	1.88
233	1/0	6519	2158	3.02	2051	3.24
33	1/0	9609	4063	2.37	4173	2.30
16	1/0	3093	**	----	----	----
237	1/0	16418	2986	5.50	2977	5.51
228	10/0	481	668	0.72	467	1.03
40	10/0	1705	930	1.83	697	2.45
6	0/1	207	168	1.23		
11	0/1	209	155	1.35		
14	0/1	219	236	0.93		

TABLE VII
BASELINE DATA CORRELATION (cont'd)

SPEC	TYPE	N_f	N_{PRED}	N_f/N_{PRED}	N_{PRED}^*	N_f/N_{PRED}^*
8	0/1	413	427	0.97		
13	0/1	846	1022	0.83		
241	0/1	1940	2022	0.96		
238	0/1	4619	2842	1.63		
222	0/10	224	581	0.39		
41	0/10	283	276	1.03		
1	1/1	156	165	0.95	154	1.01
2	1/1	238	273	0.87	259	0.92
32	1/1	358	522	0.69	495	0.72
9	1/1	959	699	1.37	727	1.32
15	1/1	1288	1259	1.02	1193	1.08
229	1/1					
28	10/10	115	105	1.10	116	0.99
31	10/10	199	144	1.38	155	1.28
230	10/10	331	450	0.74	451	0.73

* PREDICTED LIFE VALUE CALCULATED USING CYCLIC CREEP CP LINE

** COULD NOT ACCURATELY PARTITION

TABLE VIII
UNBALANCED STRAIN HOLD TESTS - PARTITIONED DATA

TEST	TYPE	$\Delta\epsilon_{TOT}^1$	$\Delta\epsilon_{in}^1$	$\Delta\epsilon_{PP}^1$	$\Delta\epsilon_{CP}^1$	$\Delta\epsilon_{CC}^1$	σ_{TEN}^2	N_f
227	10/1	1.40	.292	.198	.042	.052	144.0	455
223	10/1	1.20	.158	.113	.025	.021	118.0	945
226	1/10	1.40	.221	.158	.009	.054	165.0	349
225	1/10	1.20	.162	.114	.006	.042	150.0	464

1) % TEST STRAIN

2) KSI

TABLE IX
INTERMEDIATE STRAIN HOLD TESTS - PARTITIONED DATA

TEST	TYPE	$\Delta\epsilon_{TOT}^1$	ϵ_{HOLD}^1	$\Delta\epsilon_{in}^1$	$\Delta\epsilon_{PP}^1$	$\Delta\epsilon_{CP}^1$	$\Delta\epsilon_{PC}^1$	σ_{TEN}^2	N_f
242	i1/0	1.80	+0.80	.422	.371	.051	.000	163.0	472
244	i1/0	1.60	+0.70	.266	.227	.039	.000	154.0	447
246	i1/0	1.80	+0.70	.412	.347	.065	.000	170.0	253
247	0/i1	1.80	-0.70	.356	.298	.000	.0579	172.0	263

1) % STRAIN

2) KSI

TABLE X
LOW RATE STRAIN CYCLE TESTS (.05 CPM) - PARTITIONED DATA

SPEC	$\Delta\epsilon_{TOT}^4$	$\Delta\epsilon_{in}^4$	f_{PP}	f_{CC}	σ_{TEN}^5	N_f
23 ¹	1.84	.450	0.96	.04	161.0	110
24	1.74	.350			168.0	159
20	1.59	.250			161.0	301
25	1.46	.180			145.0	282
34 ²	1.30	.120	1.00	0.00	137.0	526
19 ³	1.17	.100	1.00	0.00	117.0	1138

1) PARTITIONED FROM RESULTS OF SPEC. 249

2) PARTITIONED FROM RESULTS OF SPEC. 250

3) PARTITIONED FROM RESULTS OF SPEC. 248

<u>0.05 cpm</u>			<u>20 cpm</u>		
SPEC	$\Delta\epsilon_{in}^4$	$\Delta\sigma_{TOT}^5$	$\Delta\epsilon_{in}^4$	$\Delta\sigma_{TOT}^5$	f_{CC}
249	.450	375	.432	373	.04
250	.030	336	.035	335	.00
248	.103	346	.136	341	.00

4) % STRAIN

5) KSI

TABLE XI
VARIABLE RATE STRAINCYCLE - PARTITIONED DATA

SPEC	TYPE	$\Delta\epsilon_{TOT}$	$\Delta\epsilon_{in}$	f_{PP}	f_{ij}	σ_{TEN}	N_f
251	FAST-SLOW	1.4	.098	.88	.12	161.0	636
252	SLOW-FAST	1.4	.066	.88	.12	166.0	194

TABLE XII
VERIFICATION TESTS - SRP LIFE PREDICTION

SPEC	TYPE	N_{PRED}	N_f	N_f/N_{PRED}
227	10/1	302	455	1.51
223	10/1	616	945	1.53
226	1/10	400	349	0.87
225	1/10	557	464	0.83
242	11/0	287	472	1.64
244	11/0	455	447	0.98
246	11/0	286	253	0.88
247	0/11	191	263	1.38
23	.05 cpm	268	110	0.41
34	.05 cpm	1290	526	0.41
15	.05 cpm	1582	1138	0.72
251	FAST-SLOW	907	636	0.70
252	SLOW-FAST	1976	194	0.10

TABLE XIII

LIFE PREDICTION - VALIDATION TESTS - STRESS/TIME EQUATIONS

SPEC	TYPE	N_{PRED}	N_f	N_f/N_{PRED}
227	10/1	354	455	.78
223	10/1	928	945	.98
226	1/10	342	349	.98
225	1/10	685	464	1.47
242	11/0	481	472	1.02
244	11/0	829	447	1.85
246	11/0	315	253	1.24
247	0/11	279	263	1.06
23	.05 cpm	188	110	.59
24	.05 cpm	145	159	1.10
20	.05 cpm	188	301	1.60
25	.05 cpm	341	282	.83
34	.05 cpm	459	526	1.15
19	.05 cpm	936	1138	1.22
51	FAST/SLOW	464	636	1.37
252	SLOW/FAST	156	194	.81

APPENDIX I
TABLE I
PHASE I TEST DATA

SPEC	TYPE HRSC	$\Delta\epsilon_{TOT}^1$	$\Delta\epsilon_{in}^1$	σ_{TEN}^2	σ_{MEAN}^2	N_f
21	20 cpm	2.20	.7900	180.0	-5.0	203
17	20 cpm	2.00	.5300	178.0	-8.5	234
18	20 cpm	1.80	.4080	175.0	-5.5	307
224	20 cpm	1.60	.2500	168.0	-4.0	415
22	20 cpm	1.60	.3110	168.0	-2.5	461
240	20 cpm	1.60	.2850	161.1	-6.2	463
26	20 cpm	1.40	.2167	156.0	-4.0	784
27	20 cpm	1.20	.1040	140.0	-3.0	1629
29	20 cpm	1.00	.0177	116.0	-8.5	5158
30	20 cpm	0.90	.0116	107.0	-9.0	16215
234	20 cpm	0.90	.0130	99.0	-17.4	19160
235	20 cpm	0.90	.0085	99.2	-15.0	22364
239	20 cpm	0.88	.0130	106.7	-6.9	28697

1) PERCENT STRAIN

2) KSI

SPEC	TYPE TSHC	$\Delta\epsilon_{TOT}^1$	$\Delta\epsilon_{in}^1$	σ_{TEN}^2	σ_{MEAN}^2	N_f
245	1/0	2.00	.6570	171.0	-11.5	171
5	1/0	1.80	.5220	161.0	-13.0	255
10	1/0	1.60	.2970	160.0	-15.5	257
7	1/0	1.40	.2060	138.0	-20.0	748
12	1/0	1.20	.0893	129.0	-18.5	1289
39	1/0	1.10	.0890	108.0	-23.0	1781
38	1/0	1.00	.0490	101.0	-23.5	5013
233	1/0	1.00	.0605	89.3	-34.6	6519
33	1/0	1.00	.0380	82.8	-38.1	9609
237	1/0	0.90	.0459	70.3	-40.8	16418
228	10/0	1.40	.1850	130.0	-30.5	481
40	10/0	1.20	.1260	108.0	-35.0	1705

APPENDIX I

TABLE I

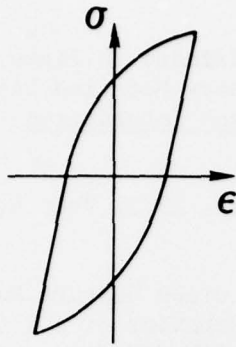
PHASE I TEST DATA (cont'd.)

SPEC	TYPE CSHT	$\Delta\epsilon_{TOT}^1$	$\Delta\epsilon_{in}^1$	σ_{TEN}^2	σ_{MEAN}^2	N_f
6	0.1	1.80	.4290	178.0	-1.5	207
11	0/1	1.60	.4680	162.0	.5	209
14	0/1	1.60	.3240	177.0	1.5	219
8	0/1	1.40	.1920	165.0	3.5	413
13	0/1	1.20	.0979	156.0	8.0	846
241	0/1	1.10	.0490	141.0	5.6	1940
16	0/1	1.00	.0103	124.0	.5	3093
238	0/1	0.90	.0280	127.4	13.0	4619
222	0/10	1.40	.1359	176.0	10.5	224
41	0/10	1.20	.1850	164.0	23.5	283
SPEC	TYPE BHST	$\Delta\epsilon_{TOT}^1$	$\Delta\epsilon_{in}^1$	σ_{TEN}^2	σ_{MEAN}^2	N_f
1	1/1	1.80	.5500	181.0	-7.5	156
2	1/1	1.60	.3490	170.0	-7.0	238
32	1/1	1.40	.2010	150.0	-11.0	358
9	1/1	1.20	.1220	135.0	-9.5	959
15	1/1	1.00	.0780	117.0	-9.5	1288
229	1/1	0.90	.0245	95.2	-16.4	5277
28	10/10	1.80	.7010	179.0	-7.0	115
31	10/10	1.40	.4970	158.0	-6.5	199
230	10/10	1.20	.1572	142.0	-9.0	331

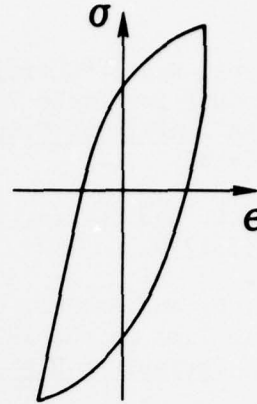
REFERENCES

1. Greenstreet, W. L., et al, "Time-Dependent Fatigue of Structural Alloys" 1977, ORNL Report 5073.
2. Manson, S. S., Halford, G. R., and Hirschberg, M. H., "Creep-Fatigue Analysis by Strainrange Partitioning", Symposium on Design for Elevated Temperature Environment, ASME, 1971, pp. 12-28. (NASA TM X -67838, 1971).
3. Saltsman, J. F. and Halford, G. R., "Application of Strainrange Partitioning to the Prediction of Creep Fatigue Lives of AISI Types 304 and 316 Stainless Steel", 1976, NASA TM X-71898.
4. Saltsman, J. F. and Halford, G. R., "Application of Strainrange Partitioning to the Prediction of MPC Creep-Fatigue Data for 2 1/4 Cr-1 Mo Steel", 1976, NASA TM X-73474.
5. Kortovich, C. S., "Strainrange Partitioning Behavior of Coated and Uncoated Rene 80 in Ultrahigh Vacuum", April 1976, NASA CR-135003.
6. Hirschberg, M. H. and Halford, G. R., "Strainrange Partitioning - A Tool for Characterizing High Temperature Low-Cycle Fatigue", 1975, NASA TM X-71691.
7. Menon, M. N., "Life Prediction Techniques for Analyzing Creep-Fatigue Interaction in Advanced Nickel-Base Superalloys", 1976, Air Force Materials Laboratory TR-76-172.
8. Menon, M. N., "Metallographic Characterization of Rene 95 Forgings", 1973, Air Force Materials Laboratory TR-73-180.
9. Menon, N. M. and Reimann, W. H., Met. Trans., 1975, Vol. 6A, pp 1075-1085.
10. Menon, M. N. and Reimann, W. H., J. Matls. Science, 1975, Vol. 10, pp. 1571-1581.
11. Slot, T., Stentz, R. H., and Berling, J. T., "Controlled Strain Testing Procedures", Manual on Low Cycle Fatigue Testing, ASTM STP 465, 1969, pp. 100-128.
12. Manson, S. S., Halford, G. R., and Nachtigal, A. J., "Separation of the Strain Components for Use in Strainrange Partitioning", Symposium on Advances in Design for Elevated Temperature Environment, ASME, 1975, pp. 17-28. (NASA TM X-71737, 1975).
13. Annis, C. G., Van Wanderham, M. C., and Wallace, R. M., "Strainrange Partitioning Behavior of an Automotive Turbine Alloy", 1976, NASA CR-134974.

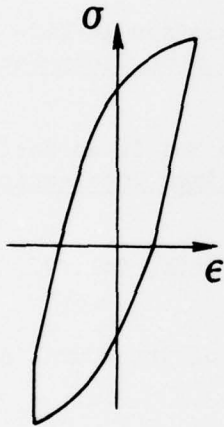
14. Ostergren, W.J., "Correlation of Hold Time Effects in Elevated Temperature Low Cycle Fatigue Using a Frequency Modified Damage Function", ASME-MPC Symposium on Creep-Fatigue Interaction, 1976, pp. 179-185.
15. Lord, D.C. and Coffin, L.F., Jr., *Met. Trans.*, 1973, Vol. 4, No. 7, pp. 1643-1770.
16. Krempl, E. and Walker, C.D., "The Effect of Creep Rupture Ductility and Hold Time on the 1000°F Strain-Fatigue Behavior of a 1 Cr-1 Mo-.25V Steel", Fatigue at High Temperature, 1969, ASTM STP 459, p. 75.
17. Conway, J.B., "Development of a Standard Methodology for the Correlation and Extrapolation of Elevated Temperature Creep and Rupture Data: Volume I, A Summary of State of the Art Review and Workshop", to be published as Electric Power Research Institute Report (NTIS listing).
18. Conway, J.B., "Pre-Analysis Assessment of Creep and Rupture Data", to be published in the Proceedings of the ASME-CSME Pressure Vessel and Piping Conference, Montreal, Canada, June 1978.
19. Coffin, L. F., "The Concept of Frequency Separation in Life Prediction for Time-Dependent Fatigue", ASME-MPC Symposium on Creep-Fatigue Interaction, 1976, pp. 349-363.
20. Majumdar, S., Maiya, P.S., "A Damage Equation for Creep-Fatigue Interaction", ASME-MPC Symposium on Creep-Fatigue Interaction, 1976, pp. 323-336.
21. Tomkins, B., *J. Engineering Mat. and Tech.*, 1975, Vol. 97, pp. 289-297.
22. Manson, S.S., et al, "Time Dependent Fatigue of Structural Alloys", ORNL Report 5073, 1977, pp. 245-307.



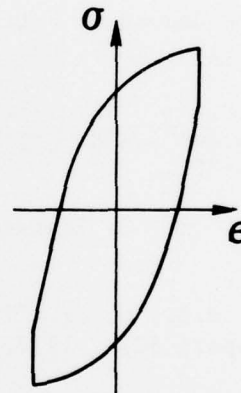
HIGH RATE STRAIN CYCLE
(CONTINUOUSLY CYCLING)



TENSILE STRAIN HOLD CYCLE



**COMPRESSIVE STRAIN
HOLD CYCLE**



BALANCED STRAIN HOLD CYCLE

Fig. 1 Hysteresis loops for the four baseline test cycles.

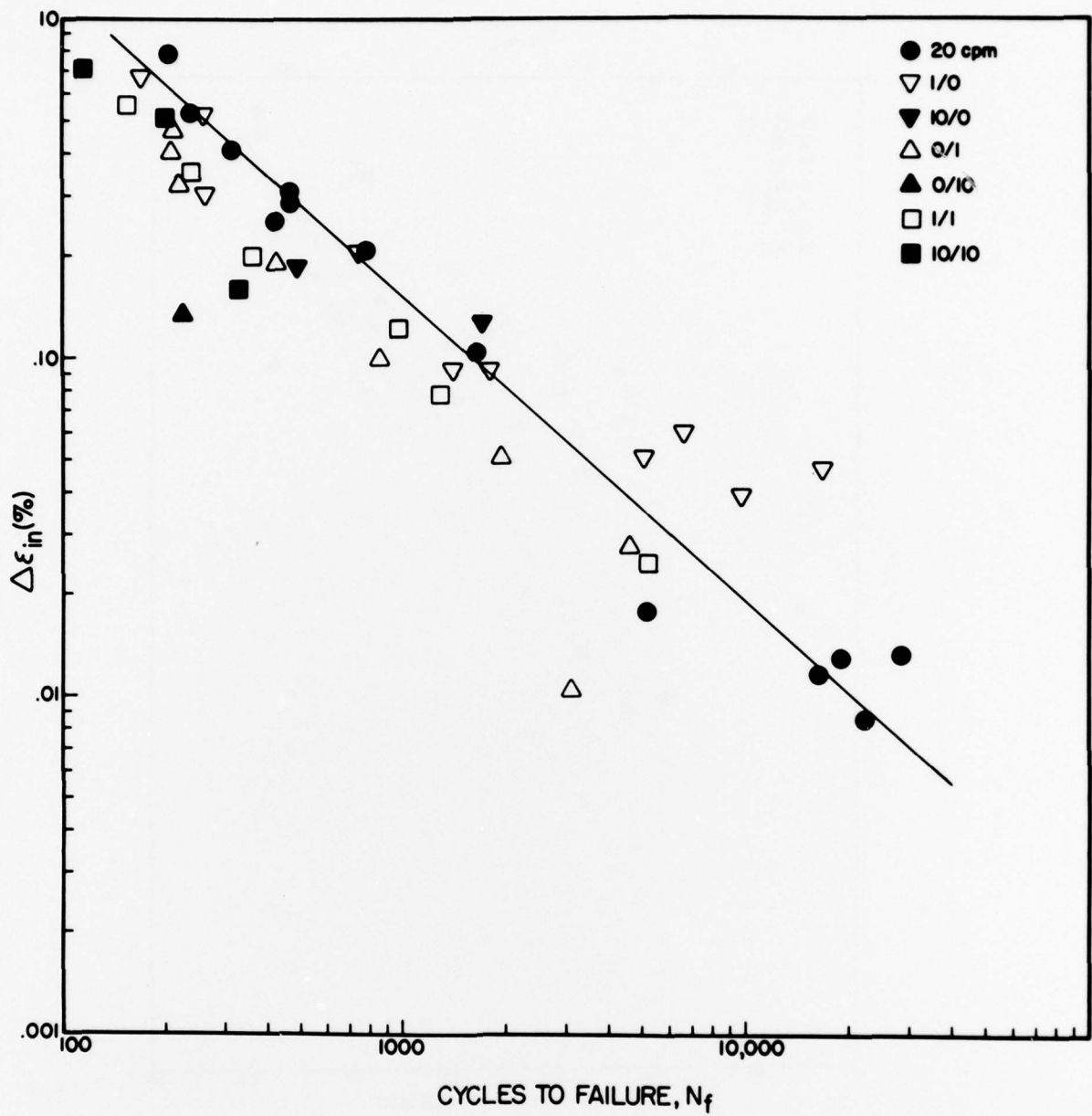


Fig. 2 Low cycle fatigue data for Rene 95 baseline strain controlled tests at 922K (1200°F). The line shown is the Manson-Coffin relationship for 20 cpm tests.

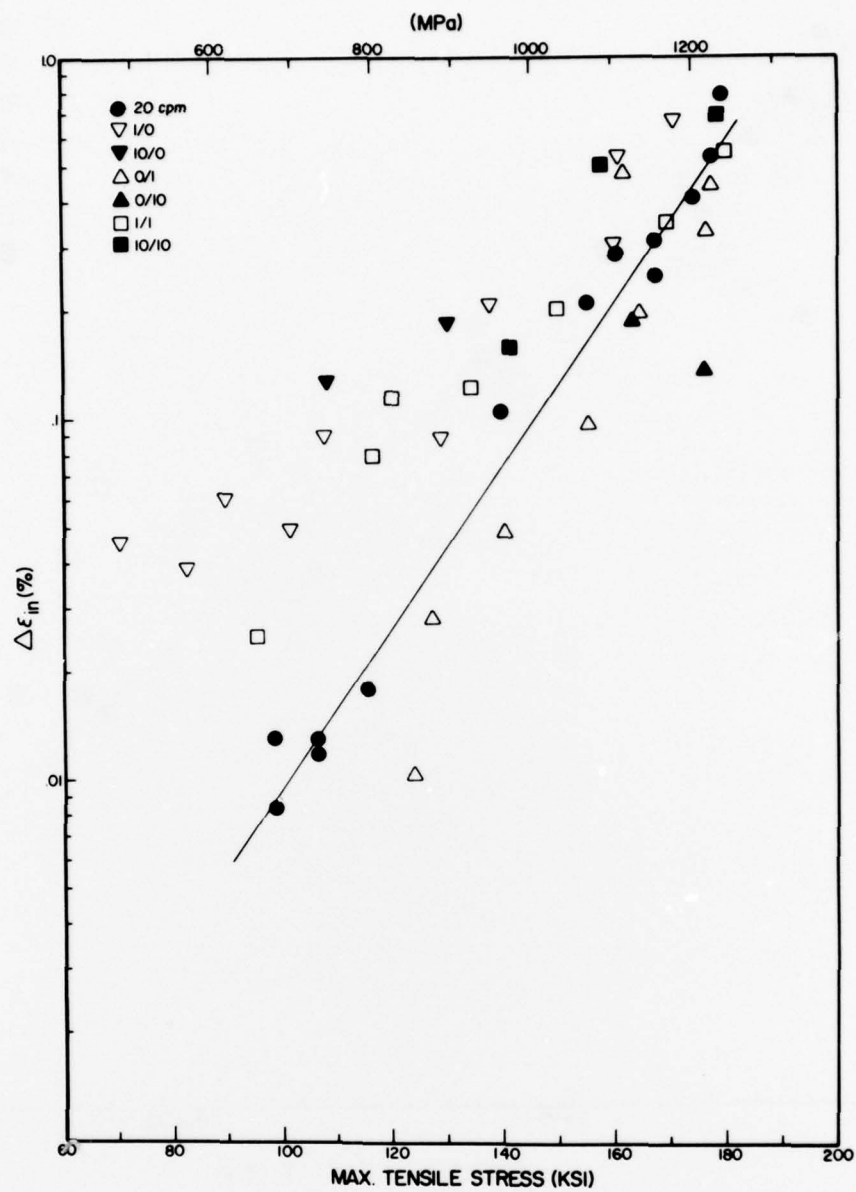


Fig. 3 Relationship of maximum tensile stress to inelastic strainrange for baseline tests. Best fit line constructed for 20 cpm data.

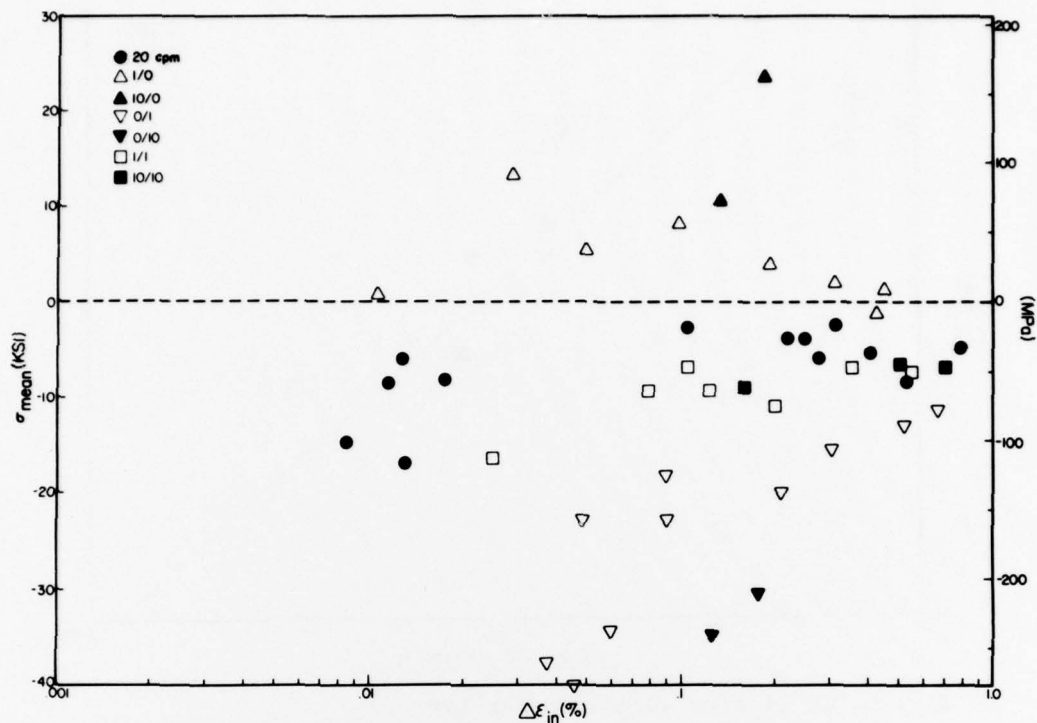


Fig. 4 Relationship of mean stress

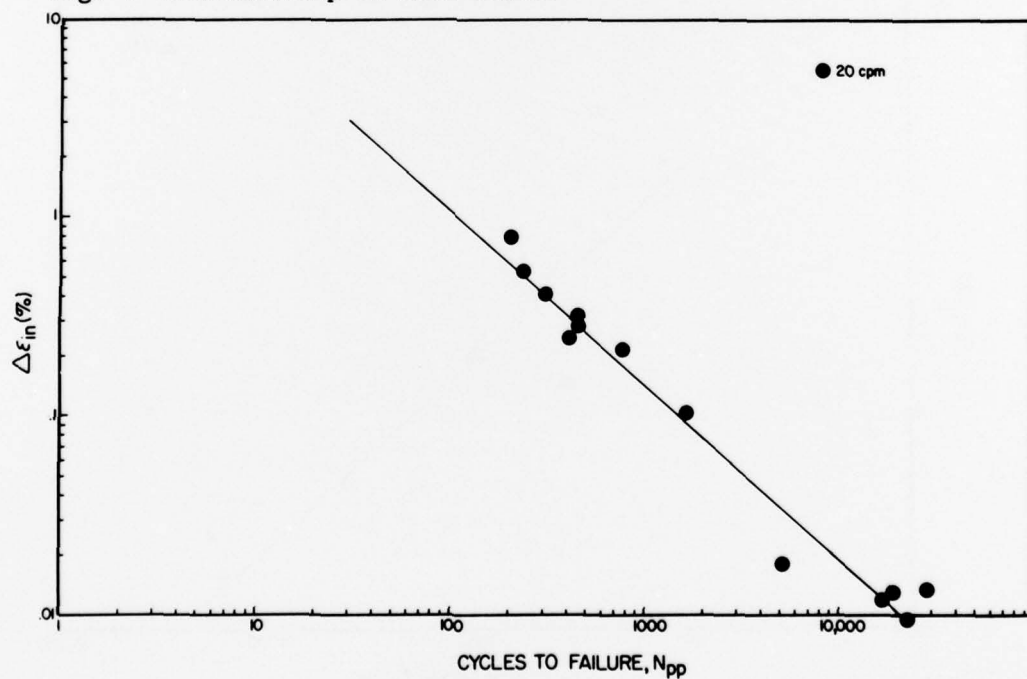


Fig. 5 PP life relationship for Rene 95

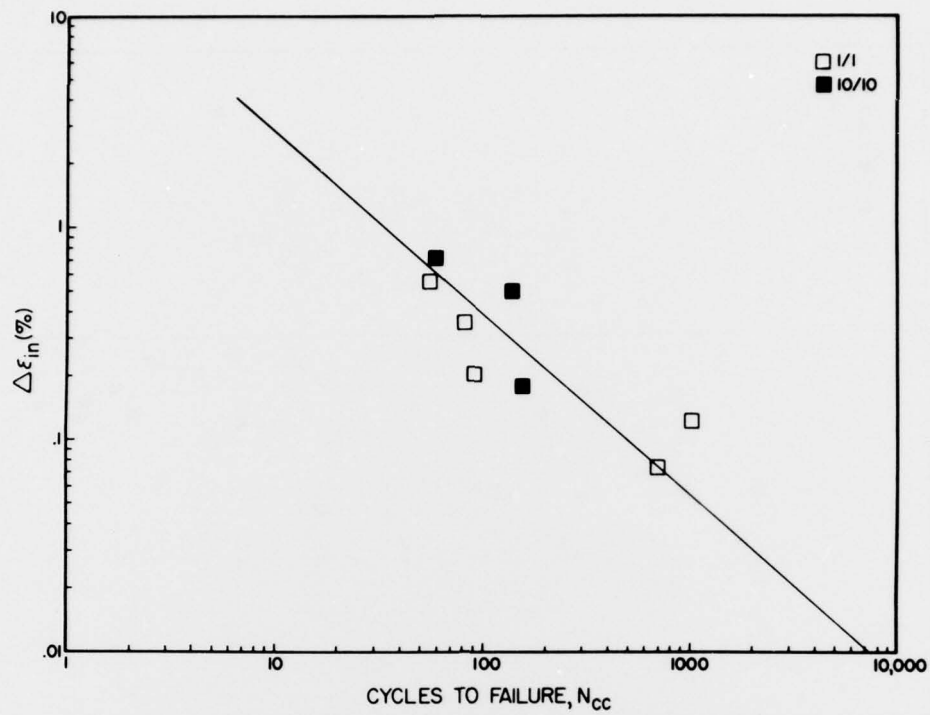


Fig. 6 CC life relationship for Rene 95

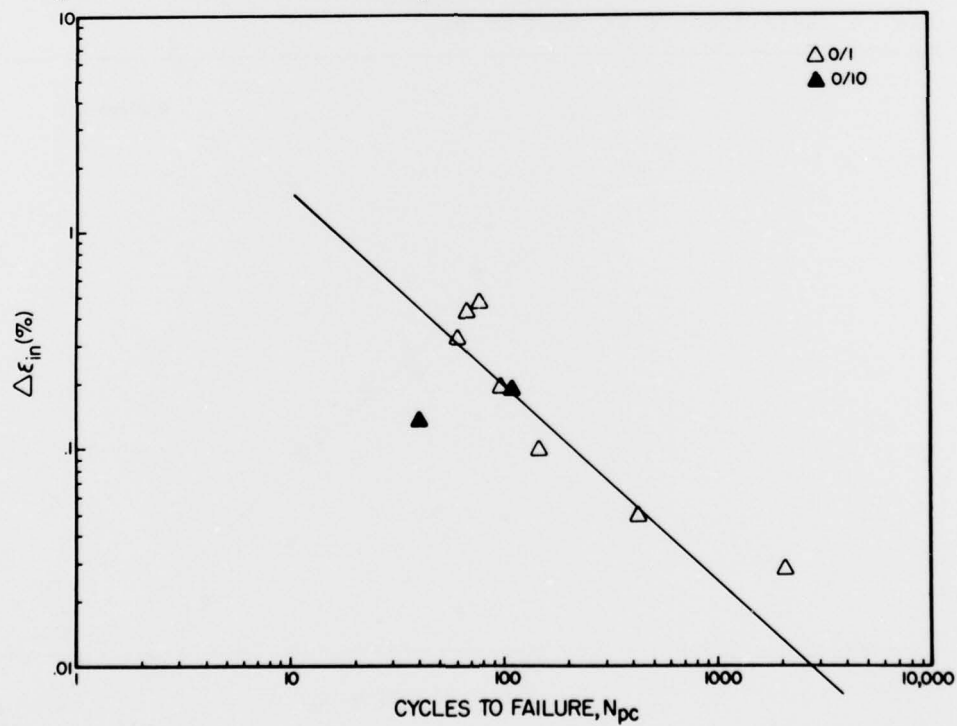


Fig. 7 PC life relationship for Rene 95

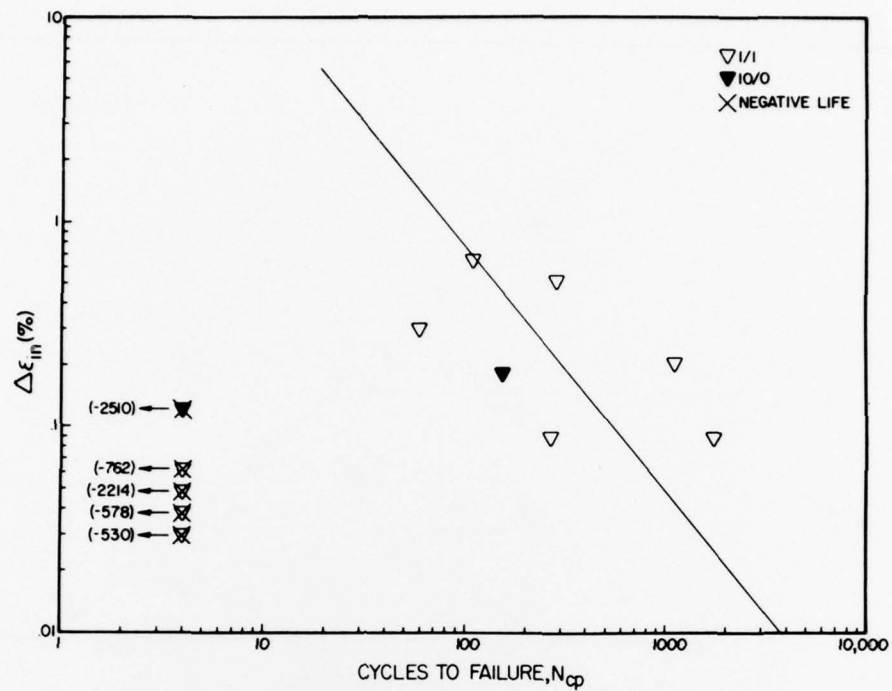


Fig. 8 CP life relationship for Rene 95 based on positive N_{CP} data only.

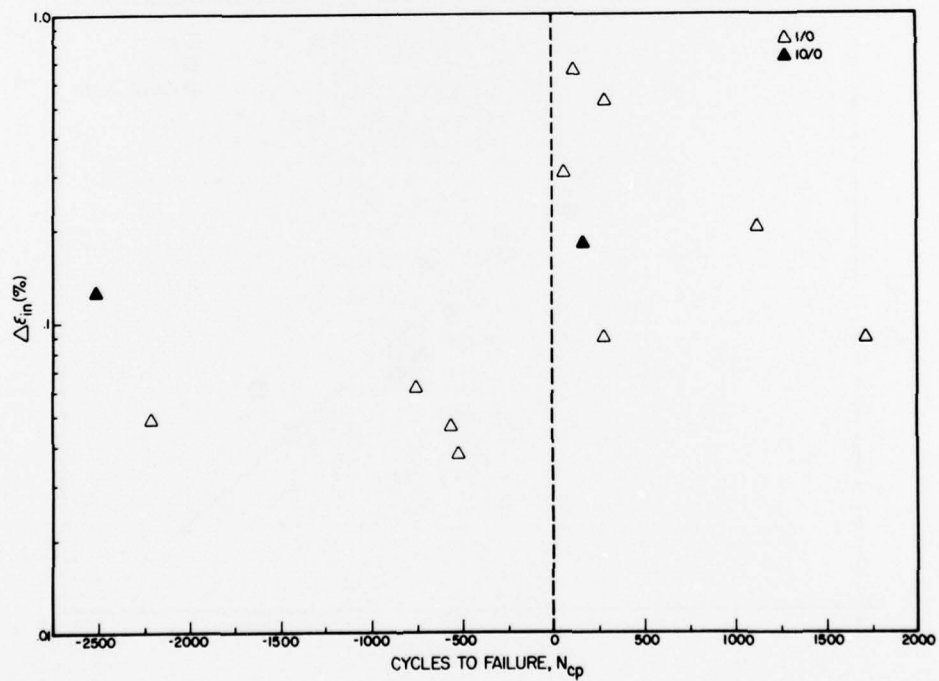


Fig. 9 Semi-logarithmic plot of N_{CP} data versus $\Delta\epsilon_{in}$ showing calculated negative N_{CP} lives.

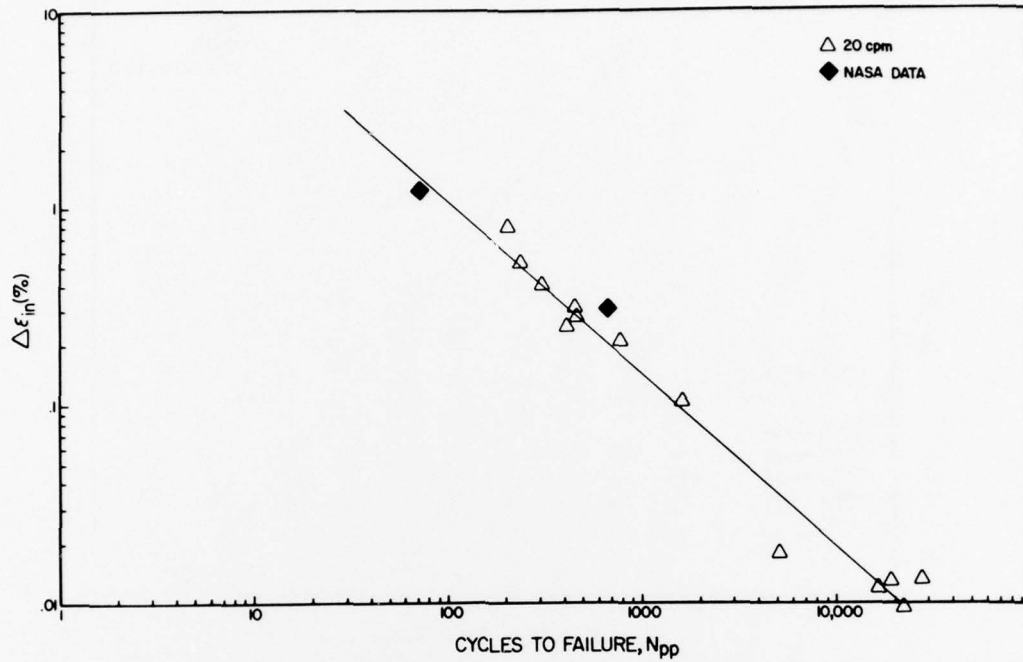


Fig. 10 Comparison of NASA PP data with baseline PP relationship

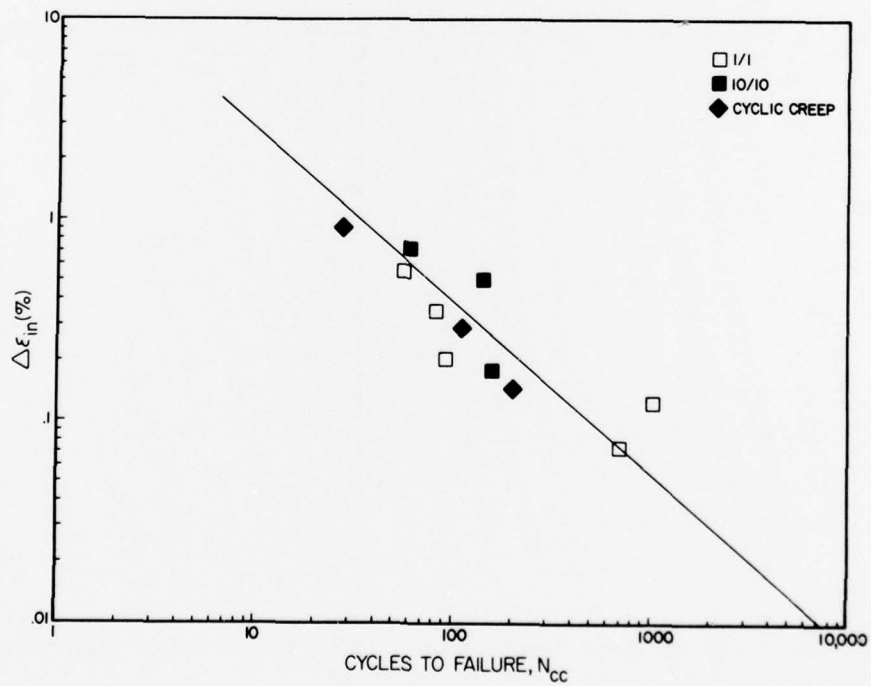


Fig. 11 Comparison of balanced cyclic creep data with the baseline CC relationship.

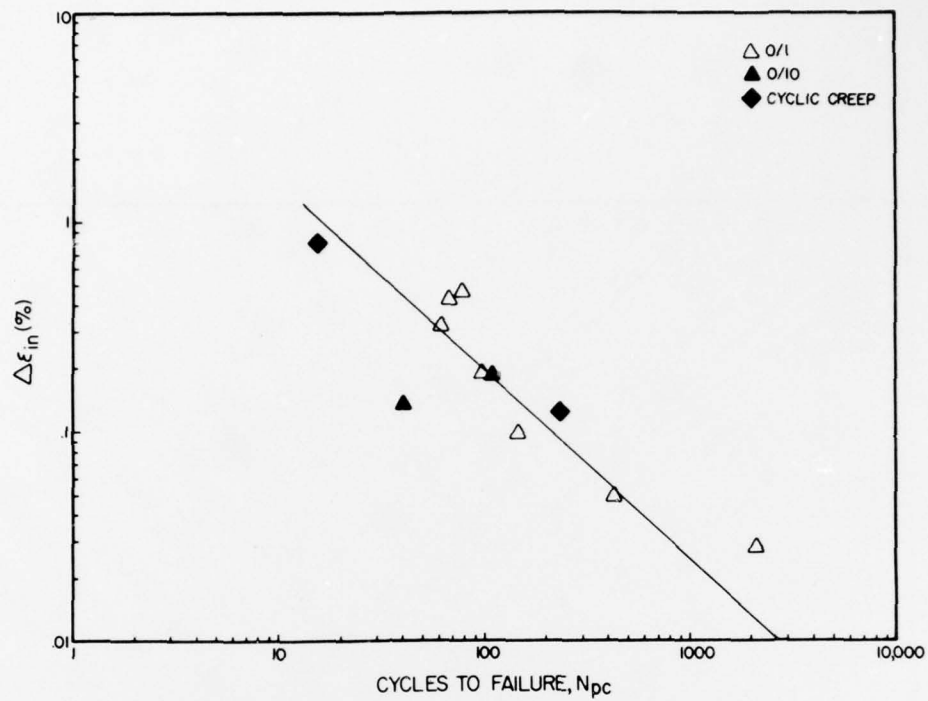


Fig. 12 Comparison of compressive cyclic creep data with the baseline PC relationship.

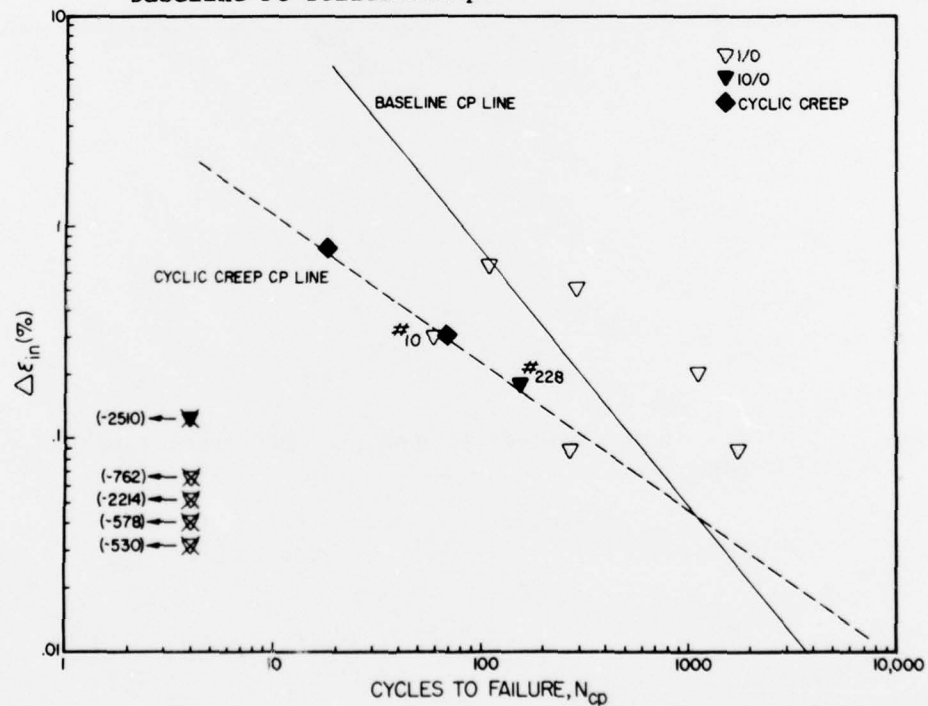


Fig. 13 Comparison of tensile cyclic creep data with the baseline CP relationship, and construction of the cyclic creep CP line.

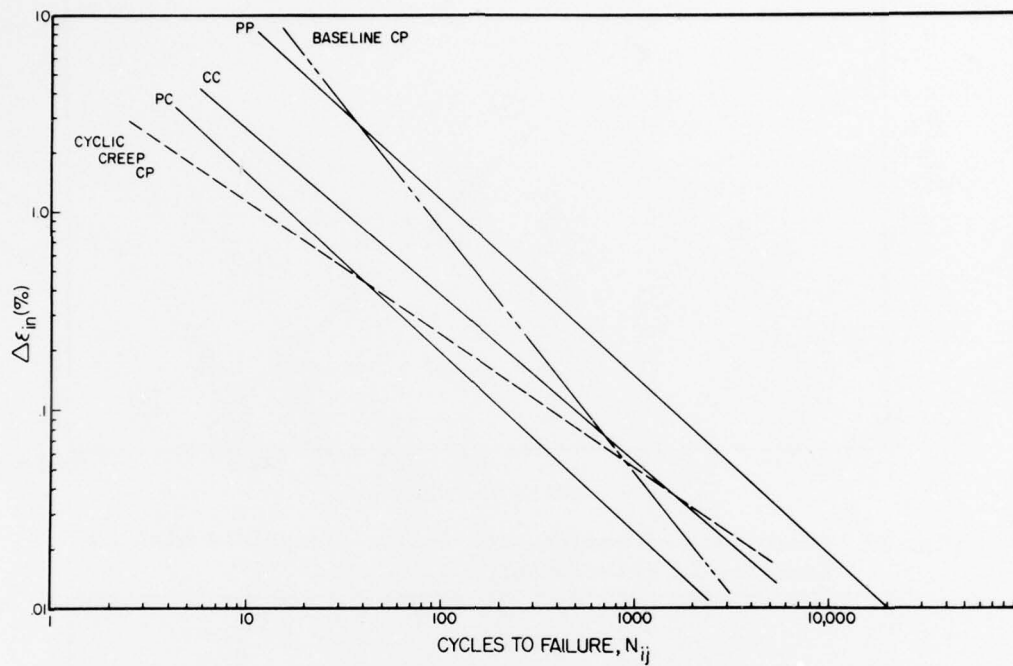


Fig. 14 Summary of partitioned strainrange-life relationships for Rene 95.

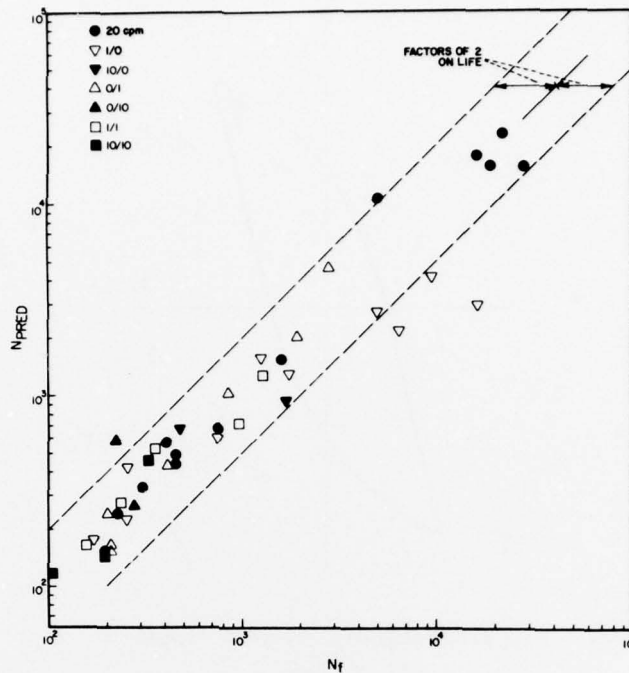


Fig. 15 Comparison of observed and predicted life for baseline tests.

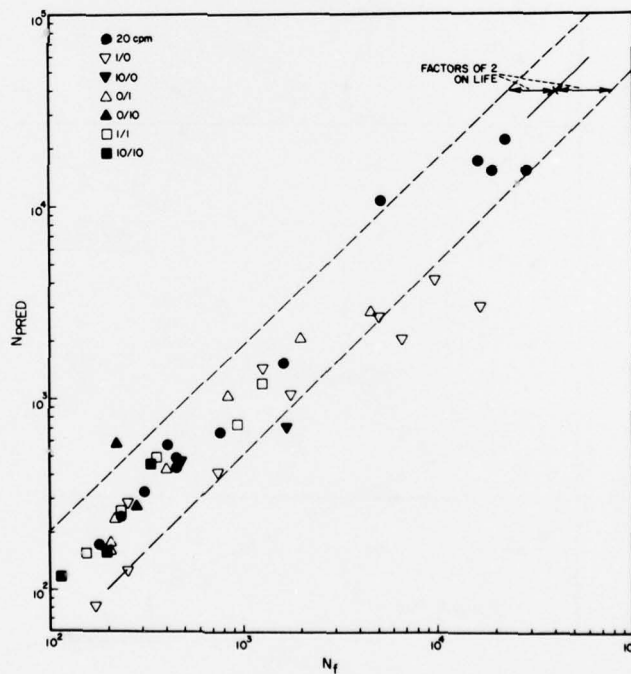
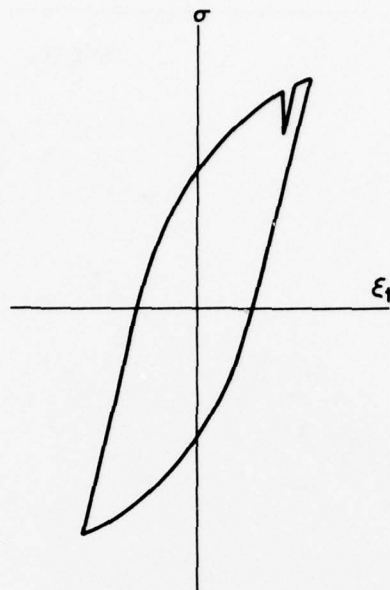


Fig. 16 Comparison of observed and predicted life for baseline tests based on cyclic creep CP line.



INTERMEDIATE STRAIN HOLD CYCLE

Fig. 17 Illustration of intermediate strain hold cycle

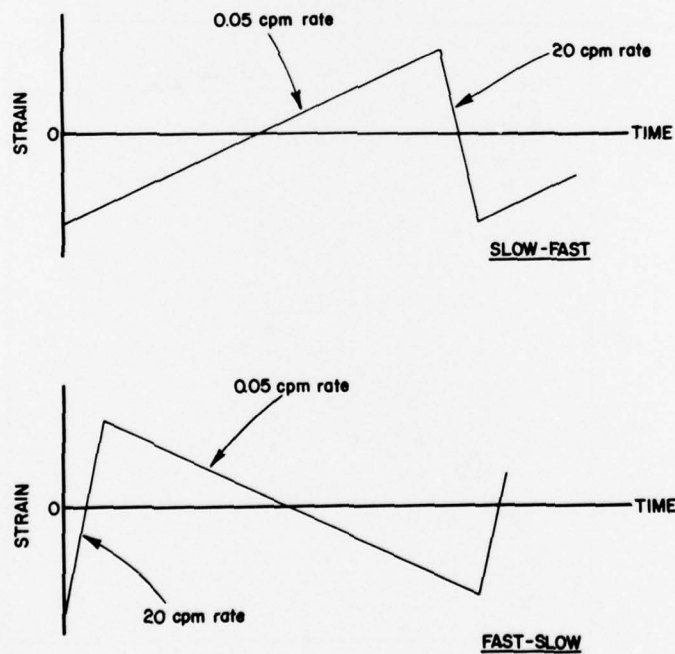


Fig. 18 Total strain versus time waveform for fast-slow and slow-fast tests.

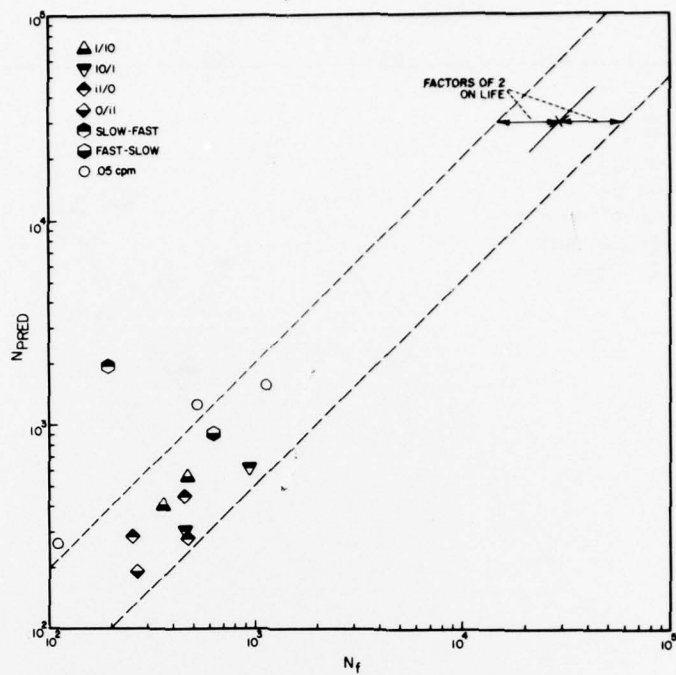


Fig. 19 Comparison of observed and predicted life for validation tests based on baseline SRP relationships.

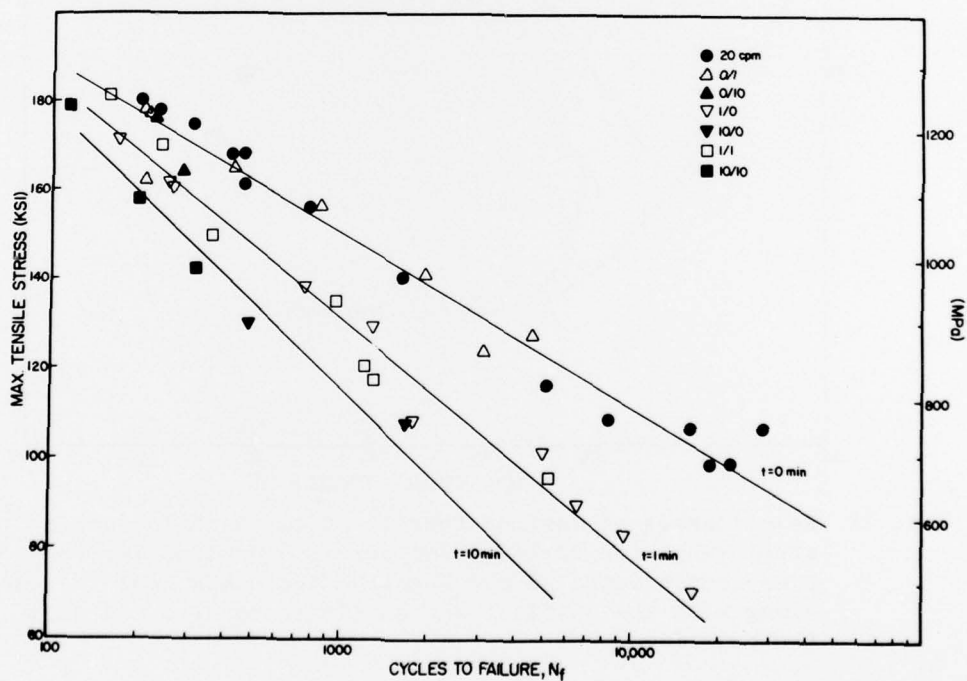


Fig. 20 Relationship of LCF life to maximum tensile stress for baseline tests with different hold times in tension.

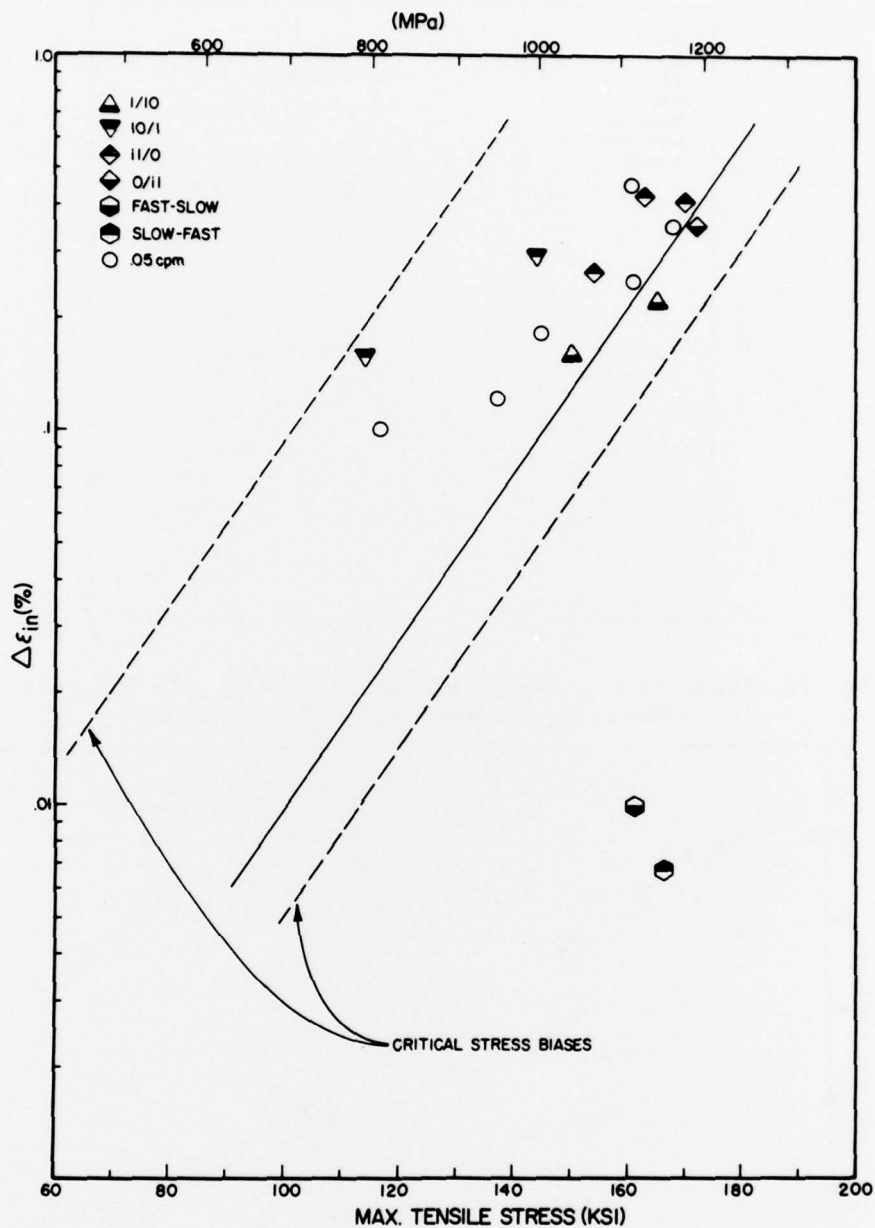


Fig. 21 Relationship of maximum tensile stress with inelastic strainrange for verification tests. The line for the time independent, 20 cpm baseline tests has been included along with the critical stress limits constructed from the baseline data.

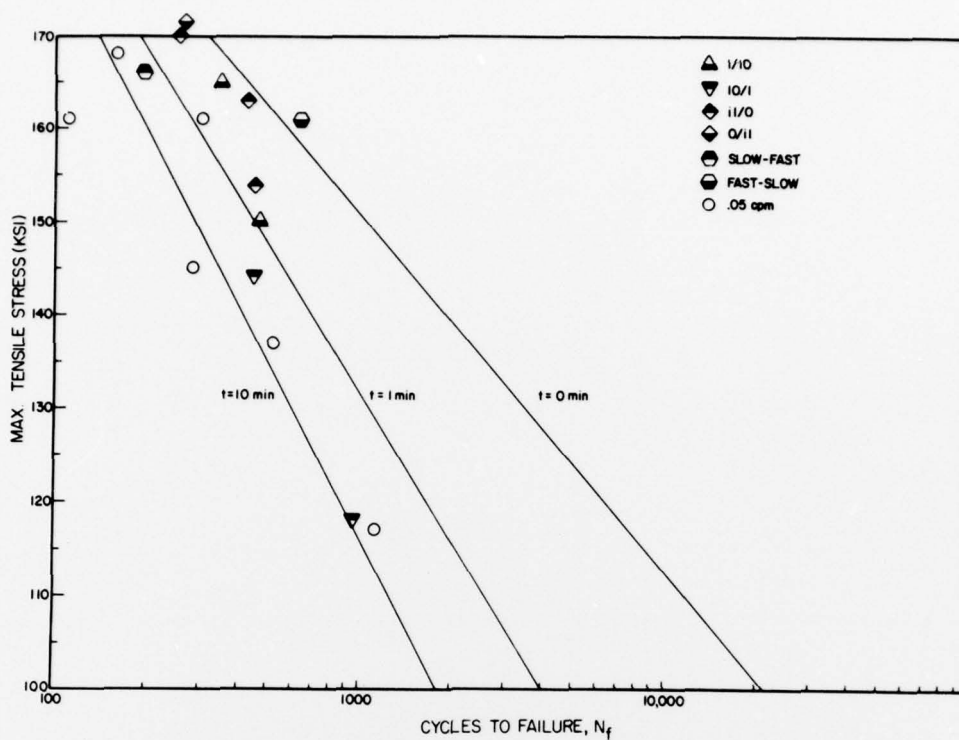


Fig. 22 Comparison of verification test data with the maximum tensile stress-tensile hold time correlation developed for the baseline tests.

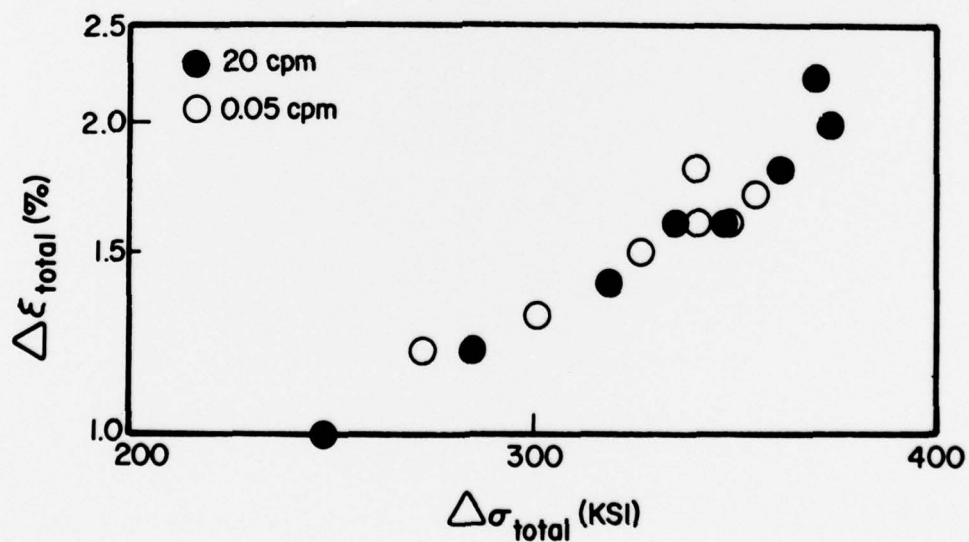


Fig. 23 Stressrange versus total strainrange for 20 cpm and 0.05 cpm continuously cycling tests.